



THE UNIVERSITY *of* EDINBURGH

Edinburgh Research Explorer

Faint Standards for ZYJHK from the UKIDSS and VISTA Surveys

Citation for published version:

Leggett, SK, Cross, NJG & Hambly, NC 2020, 'Faint Standards for ZYJHK from the UKIDSS and VISTA Surveys', *Monthly Notices of the Royal Astronomical Society*. <https://doi.org/10.1093/mnras/staa310>

Digital Object Identifier (DOI):

[10.1093/mnras/staa310](https://doi.org/10.1093/mnras/staa310)

Link:

[Link to publication record in Edinburgh Research Explorer](#)

Document Version:

Peer reviewed version

Published In:

Monthly Notices of the Royal Astronomical Society

General rights

Copyright for the publications made accessible via the Edinburgh Research Explorer is retained by the author(s) and / or other copyright owners and it is a condition of accessing these publications that users recognise and abide by the legal requirements associated with these rights.

Take down policy

The University of Edinburgh has made every reasonable effort to ensure that Edinburgh Research Explorer content complies with UK legislation. If you believe that the public display of this file breaches copyright please contact openaccess@ed.ac.uk providing details, and we will remove access to the work immediately and investigate your claim.



Faint Standards for *ZYJHK* from the UKIDSS and VISTA Surveys

S. K. Leggett,¹* Nicholas J. G. Cross,² and Nigel C. Hambly²

¹*Gemini Observatory Northern Operations*

²*Institute for Astronomy, University of Edinburgh, Royal Observatory, Blackford Hill, Edinburgh EH9 3HJ, UK*

Accepted XXX. Received YYY; in original form ZZZ

ABSTRACT

The currently defined “UKIRT Faint Standards” have *JHK* magnitudes between 10 and 15, with $K_{\text{median}} = 11.2$. These stars will be too bright for the next generation of large telescopes. We have used multi-epoch observations taken as part of the UKIRT Infrared Deep Sky Survey (UKIDSS) and the Visible and Infrared Survey Telescope for Astronomy (VISTA) surveys to identify non-variable stars with *JHK* magnitudes in the range 16 – 19. The stars were selected from the UKIDSS Deep Extragalactic Survey (DXS) and Ultra Deep Survey (UDS), the WFCAM calibration data (WFCAM-CAL08B), the VISTA Deep Extragalactic Observations (VIDEO) and UltraVISTA. Sources selected from the near-infrared databases were paired with the Pan-STARRS Data Release 2 of optical to near-infrared photometry and the Gaia astrometric Data Release 2. Colour indices and other measurements were used to exclude sources that did not appear to be simple single stars. From an initial selection of 169 sources, we present a final sample of 81 standard stars with *ZYJHK* magnitudes, or a subset, each with 20 to 600 observations in each filter. The new standards have $K_{S_{\text{median}}} = 17.5$. The relative photometric uncertainty for the sample is < 0.006 mag and the absolute uncertainty is estimated to be $\lesssim 0.02$ mag. The sources are distributed equatorially and are accessible from both hemispheres.

Key words: standards – methods observational – techniques photometric

1 INTRODUCTION

Optical and infrared sky surveys have produced data with excellent astrometric and photometric precision. In 2019, we are benefiting from data releases by ground- and space-based surveys that were many years in the planning.

The Gaia mission (Gaia Collaboration et al. 2016) issued Data Release 2 on 2018 April 25. This release contains astrometric results for about 1.7 billion stars brighter than optical magnitude 21; parallaxes and proper motions are given for about 1.3 billion of these (Gaia Collaboration et al. 2018). The Sloan Digital Sky Survey (SDSS, York et al. 2000) and the Panoramic Survey Telescope & Rapid Response System (Pan-STARRS, Chambers et al. 2016) have imaged large areas of the Northern sky in blue/green to far-red/near-infrared filters. Tonry et al. (2012) give transformations between the SDSS and Pan-STARRS photometric systems. After transformation, the rms difference between the SDSS and Pan-STARRS *griz* photometry is 8 mmag, following a recalibration of the SDSS photome-

try with new flat fields and zero points derived from Pan-STARRS (Finkbeiner et al. 2016). This is consistent with Padmanabhan et al. (2008) who report a relative calibration accuracy of 0.7 – 1.3% for each filter in the SDSS.

Several near-infrared surveys of the sky have been undertaken in the last two decades. The 2-micron All Sky Survey (2MASS, Skrutskie et al. 2006) was executed between 1997 and 2001, with 1.3 m telescopes in both hemispheres providing complete sky coverage. The UKIRT Infrared Deep Sky Survey (UKIDSS, Lawrence et al. 2007) consisted of several Northern-hemisphere sub-surveys using the WFCAM camera and *ZYJHK* filters, and was executed between 2007 and 2011 on the 3.8 m UKIRT on Mauna Kea. Following UKIDSS, in 2012, the UKIRT Hemisphere Survey (UHS, Dye et al. 2018) began, and aims to provide continuous coverage in the *J* and *K* bands over the Declination range of zero to +60 degrees. A collaboration between the University of Hawaii and the United States Naval Observatory is continuing the UKIRT survey and adding the *H* band (Hodapp et al. 2018). In the Southern hemisphere, the 4.1 m Visible and Infrared Survey Telescope for Astronomy (VISTA Sutherland et al. 2015) started surveying the sky

* E-mail sleggett@gemini.edu

in 2009; the first surveys are complete or nearing completion as of 2019¹; VISTA is producing several sub-surveys using the *ZYJHKs* filters, or a subset. [González-Fernández et al. \(2018\)](#) compare the VISTA and UKIDSS photometric systems using equatorial stars observed with both cameras. The differences are small, and after transformation the rms difference between the measurement sets is 1 – 3 mmag at *JHK*.

The near-infrared surveys cover the entire sky and provide 1 – 10 sources per square arcminute on average. Such stars could be used to calibrate science data to ~10% ([González-Fernández et al. 2018](#); [Hodgkin et al. 2009](#)). Photometric standard stars are needed to calibrate data more accurately. In the near-infrared these have frequently been provided by UKIRT measurements published by [Hawarden et al. \(2001\)](#) and [Leggett et al. \(2006\)](#). The UKIRT Faint Standards (FS) cover a range in Declination of –25 to +55 degrees. They have *JHK* Vega magnitudes of 10 – 15 with $K_{\text{median}} = 11.2$ and $\sigma_{\text{median}} = 0.01$. The UKIRT FS require integration times of 1 – 10 seconds when observed on 8 m telescopes such as at the Gemini Observatory. On future telescopes with diameters three or more times larger, the integration times will be < 1 s; such short integrations are not only inefficient, they may give rise to calibration problems such as poor linearity corrections (e.g. [Leggett et al. 2006](#)).

In this paper we identify stars in the UKIDSS and VISTA surveys that are fainter than the UKIRT FS by a factor of ~100. We select sources that have a large number of repeat measurements which show them to be non-variable, and which have high precision photometric measurements. We pair the list of candidates with the Pan-STARRS and Gaia databases and use the optical and near-infrared colours to refine the sample and produce a set of well-measured and well-behaved single stars.

2 THE SURVEYS

The Northern hemisphere UKIDSS (with the WFCAM camera) and the Southern hemisphere VISTA use similar-size telescopes, and similar filters defined according to the Mauna Kea Observatories filter specifications ([Tokunaga et al. 2002](#)). Survey data generated by both telescopes are initially processed by the Cambridge Astronomy Survey Unit (CASU) and then transferred to the Wide-Field Astronomy Unit (WFAU) in Edinburgh for further processing and archiving ([Cross et al. 2012](#); [Hambly et al. 2008](#)). Table 1 gives a summary of the properties of the surveys used in this work.

Each of the surveys has a source table (e.g. `dxsSource`) which contains band-merged detections from deep images. In addition, for the surveys used here, there is a variability table (e.g. `dxsVariability`) which contains the light-curve statistics for each primary source that is detected in at least one epoch. Details of the multi-epoch table structure and processing can be found in [Cross et al. \(2009\)](#). The number of good observations for each filter and each source is given as `nGoodObs` in the variability table; these are measurements

Table 1. Overview of the Sky Survey Data

Survey Name	Area deg ²	Filters	Vega mag 5 σ Limits	Ref.
UKIDSS Deep Extragalactic Survey (DXS)	35.0	<i>JHK</i>	21 – 22	1
UKIDSS Ultra Deep Survey (UDS) ^a	0.8	<i>JHK</i>	23 – 25	1
VISTA Deep Extragalactic Observations (VIDEO)	12.0	<i>ZYJHKs</i>	24 – 25	2
VISTA UltraVISTA ^b	1.5	<i>YJHKs</i>	22 – 24	3
WFCAM Calibration WFCAMCAL08	10.4	<i>ZYJHK</i>	18 – 19	4

References: (1) [Lawrence et al. \(2007\)](#), (2) [Jarvis et al. \(2013\)](#), (3) [McCracken et al. \(2012\)](#), (4) [Ferreira Lopes et al. \(2015\)](#).

^a For the UDS, the source table aperture magnitudes are not aperture corrected and the variability table mean magnitudes are. For a sample of 30 objects, we find an average offset in photometry of 0.190 ± 0.005 , 0.202 ± 0.006 , and 0.179 ± 0.006 , at *J*, *H* and *K* respectively, such that the mean magnitudes are brighter.

^b For UltraVISTA there are differences in the aperture corrections and zeropoints used for the source table aperture magnitudes and the variability table mean magnitudes. For a sample of 19 objects we find $\text{meanMag} - \text{aperMag3} = 0.020 \pm 0.005$, 0.052 ± 0.006 , -0.025 ± 0.010 , and -0.004 ± 0.012 at *Y*, *J*, *H* and *Ks* respectively.

which are not flagged as blended, saturated, etc. using the post-processing error bit flag (`ppErrBits`), i.e. a good observation has `ppErrBits=0`². The source and variability tables share the same primary key `sourceID`.

Our goal is to identify stars that are not variable, that have well-measured *JHK* magnitudes, and are fainter than $K = 16$. Therefore we only used surveys with variability tables for all of the *J*, *H*, and *K* filters. This means we include the UKIDSS Deep Extragalactic Survey (DXS), Ultra Deep Survey (UDS) and WFCAMCAL calibration data, but do not include the UKIDSS Galactic Clusters, Galactic Plane or Large Area Surveys (GCS, GPS, LAS). Similarly we use the VISTA Deep Extragalactic Observations Survey (VIDEO) and UltraVISTA surveys, but do not include the VISTA Kilo-Degree Infrared Galaxy, Magellanic Clouds, Variables in the Via Lactea, or Hemisphere Surveys (VIKING, VMC, VVV, VHS). The DXS, UDS, WFCAMCAL and VIDEO surveys are complete. The UltraVISTA survey is being continued³ with a final data release planned for 2021⁴.

The variability flag for each source (`variableClass`) is determined from repeat measurements and is stored in the variability table ([Cross et al. 2009](#)). The value is determined by the significance of the weighted average of the intrinsic noise over the expected noise, as given by a noise model for each pointing and each band. The weighting of the intrinsic noise is based on the number of good observations: $w_f = \frac{N_{\text{obs},f} - N_{\text{min}}}{N_{\text{obs},\text{max}} - N_{\text{min}}}$, where $N_{\text{min}} = 5$ is the minimum number of observations necessary to measure variability, $N_{\text{obs},f}$ is the number of good observations in that

² <http://wsa.roe.ac.uk/ppErrBits.html>

³ <https://www.eso.org/sci/observing/PublicSurveys/sciencePublicSurveys.html#vistacycle2>

⁴ https://www.eso.org/sci/observing/PublicSurveys/docs/UltraVISTA2_SMP_03022017.pdf

¹ <https://www.eso.org/sci/observing/PublicSurveys/sciencePublicSurveys.html>

band, and $N_{obs,max}$ is the maximum number of good observations for the star in any band. The default classification is non-variable (`variableClass = 0`), and if a star has fewer than 5 good observations in all bands it will be classified as non-variable; none of the objects selected here fall into this category. If a star has fewer than 5 observations in all bands but one, that band will determine the classification. If there are hundreds of observations in one band and tens in the others, the band with hundreds will have a strong weighting compared to the others. The star is classified as variable (`variableClass = 1`) if the ratio of the weighted intrinsic noise to the expected noise is > 3 .

We adopt the mean photometric magnitudes and uncertainties given in the variability tables as the reference calibration data in this work, and not the source table aperture magnitudes, for the following reasons. In some cases, the source tables do not go as deep as the stacked variability images; this is the case for the WFCAMCAL08 database where it was important to avoid source blending for calibration purposes. For the Ultra Deep Survey the source table photometry `AperMag` is not aperture-corrected, while the variability photometry `MeanMag` is (Table 1, Section 3). For the most recently processed survey, UltraVISTA, there are small differences between the variability and source table photometry due to different aperture corrections and Vega-to-AB zeropoint corrections (Table 1, Section 3). These issues will be corrected in a forthcoming UltraVISTA release. The variability photometry is processed in the same way for all the surveys used here, and so provides a self-consistent sample.

3 THE SQL SELECTIONS

We used the WFCAM Science Archive⁵ and the VISTA Science Archive⁶ to query the DXS, UDS, UltraVISTA, VIDEO and WFCAMCAL databases. The most recent data releases available at the time of writing were used: Data Release 11 of the DXS and UDS was used, Data Release 4 for UltraVISTA, Data Release 5 for VIDEO, and WFCAMCAL08B. For all surveys we selected for the photometric source to be the same as the source in the variability catalogue and for non-variable sources, for example `SELECT FROM dxsSource AS s, dxsVariability AS v WHERE s.sourceID=v.sourceID AND v.variableClass=0`.

We selected for point sources using the surveys' morphological classifications. For the shallower surveys – DXS and WFCAMCAL – the classification scheme uses a statistic which describes how point-like each object is with respect to an empirically derived, idealized radial profile representing the point source function (PSF) for the frame (Irwin et al. 2004; Hambly et al. 2008). The deeper surveys – UDS, UltraVISTA and VIDEO – use the TERAPIX SWARP image resampling tool (Bertin et al. 2002) and the `CLASS_STAR` statistic⁷ generated by the SEXTRACTOR software (Bertin & Arnouts 1996), together with magnitude cuts in each band (Liske et al. 2003; Warren et al.

2007). We found that we could select a good-sized sample of objects (more than ten) from each of the DXS, UDS, and WFCAMCAL surveys by selecting for stars only, using `s.mergedClass=-1`. For VIDEO we relaxed the selection to stars and probable stars, with `s.mergedClass` in $(-1, -2)$, in order to get a useful sample. For UltraVISTA we found that the `mergedClass` statistic in the source table classifies all sources with multi-filter photometry as galaxies. A visual inspection of the sources in the stacked images showed that the PSFs in the *Y* and *J* images are extended. We expect that future releases of the ongoing UltraVISTA survey will include improved morphological classifications. For this work, for UltraVISTA, we selected for possible stars by using the class statistic determined from the *H* and *K* images, `s.hclassStat>0.7 AND s.kclassStat>0.7`, and we use additional profile and colour selections to separate galaxies from stars (Section 6).

We selected for precise photometry by restricting the uncertainty in the mean magnitude to ≤ 0.006 mag. The photometric uncertainties are given in the variability catalogue by the rms value of the multiple measurements (`MagRms`) and the median absolute deviation of the magnitude (`MagMAD`): we selected for sources where these values scaled as expected with `nGoodObs`, for example `(v.jMagMAD/SQRT(v.jnGoodObs - 1))<=0.004 AND (v.jMagRms/SQRT(v.jnGoodObs - 1))<=0.006`.

For the DXS, VIDEO and WFCAMCAL surveys we selected for consistency between the source and variability table magnitudes by limiting the difference to 2.5σ where σ is determined from the variability rms and the source aperture magnitude error, for example, `(s.jAperMag3 - v.jMeanMag) < 2.5 * (SQRT(s.jAperMag3err * s.jAperMag3err + (v.jMagRms/SQRT(v.jnGoodObs - 1)) * (v.jMagRms/SQRT(v.jnGoodObs - 1))))`. For the UDS and UltraVISTA surveys, where there are systematic differences between the source and variability table magnitudes (Section 2 and Table 1), we selected for objects with a small range around the average offset; for example for the UDS we used `(s.jAperMag3 - v.jMeanMag < 0.20) AND (s.jAperMag3 - v.jMeanMag > 0.18)`, and for UltraVISTA we used `((s.jAperMag3 - v.jMeanMag) <= -0.04) AND ((s.jAperMag3 - v.jMeanMag) >= -0.08)`.

A limit on target declination was also implemented. In Sections 6 and 7 we use Pan-STARRS optical data, together with the near-infrared data, to further refine the star/galaxy separation and to remove sources which may be multiple, as evidenced by unusual colours. For this reason we restricted our searches to declination $> -30^\circ$.

The constraints on brightness and number of observations in each filter varied with each survey. Sources with $K > 16$ or $K > 16.5$ were selected from the DXS, UltraVISTA and WFCAMCAL, while sources with $K > 17.5$ were selected from the deeper UDS and VIDEO surveys (Table 1). For the data to be of calibration quality, we adopt a minimum number of measurements of 20 for each object in each filter. Less than twenty *H*-band observations were obtained for some objects in the DXS, and for that survey we restricted the search to a minimum of 20 observations in *J* and *K* and 5 in *H*, in order to use the colour information. The minimum number of observations for the other surveys ranged from 20 to 100 for each filter. While the *JHK* filters

⁵ <http://wsa.roe.ac.uk>

⁶ <http://surveys.roe.ac.uk/vsa>

⁷ <https://sextractor.readthedocs.io/en/latest/ClassStar.html>

are our priority in this work, we also record the Z and Y magnitudes where available.

The SQL queries used for each survey in their complete form are given in the Appendix. The searches produced 169 sources: 34 from the DXS, 51 from the UDS, 25 from UltraVISTA, 47 from the VIDEO survey, and 12 from WFCAM-CAL.

4 THE WFCAM-UKIDSS AND VISTA PHOTOMETRIC SYSTEMS

Both WFCAM and VISTA use filters specified by the Mauna Kea Observatories system (Tokunaga et al. 2002). There are small differences in the filters as delivered, and differences in the site and telescope optics, which lead to small differences between the native UKIDSS and VISTA photometric systems. González-Fernández et al. (2018) use a large sample of reddening-free stars with photometric errors < 0.1 mag, observed with both cameras, to derive the following color transformations between VISTA and WFCAM:

$$Z_V - Z_W = -(0.037 \pm 0.008) \times (J - K)_W + (0.040 \pm 0.005)$$

$$Y_V - Y_W = -(0.010 \pm 0.003) \times (J - K)_W - (0.048 \pm 0.002)$$

$$J_V - J_W = -(0.028 \pm 0.002) \times (J - K)_W - (0.004 \pm 0.001)$$

$$H_V - H_W = -(0.037 \pm 0.001) \times (J - K)_W + (0.025 \pm 0.001)$$

$$K_{SV} - K_W = (0.017 \pm 0.003) \times (J - K)_W - (0.022 \pm 0.002)$$

VISTA survey observations are continuing, and the photometry presented here can be enhanced by future UltraVISTA data releases, hence we convert the UKIDSS photometry to the VISTA system and use that as our reference system in this work.

The UKIDSS UDS field (Data Release 11) and the VISTA VIDEO XMM-Newton field (Data Release 5) overlap by 0.1 deg in Right Ascension and 0.9 deg in Declination. A search for non-variable point sources in the common region with $\text{AperMag3err} \leq 0.006$ produced a sample of 43 stars with H and K magnitudes between 13 and 16 (no J measurements were available). Allowing for small color transformations (see above), we find a mean difference between the UDS and VIDEO survey magnitudes of 0.010 mag at H and K . These results suggest that the color-transformed standard star photometry presented in this paper is robust at the 1% level.

5 MATCHING TO PAN-STARRS AND GAIA

The coordinates of the sources produced by our SQL searches of the WFCAM and VISTA science archives, described above, were matched to Data Release 2 of the Pan-STARRS data archive⁸ and Data Release 2 of the Gaia data archive⁹, which were the most recent releases at the time of

⁸ <https://catalogs.mast.stsci.edu/>

⁹ <https://gea.esac.esa.int/archive/>

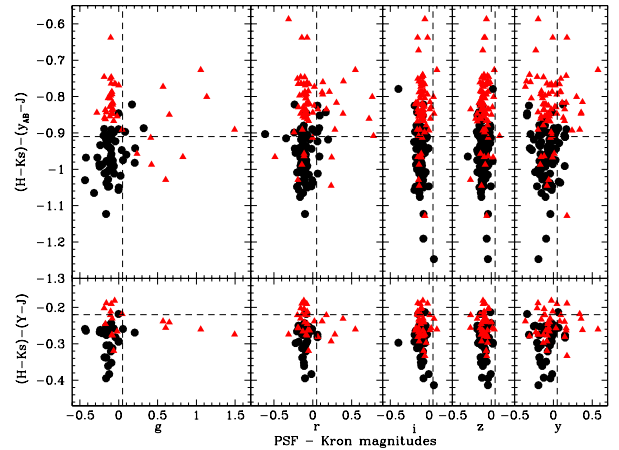


Figure 1. Red triangles are identified as possible galaxies either by the PSF – Kron magnitude or the colour index. The limits on these values are indicated by the dashed lines, see Section 6.

writing. The Pan-STARRS *grizy* magnitudes ranged from 18 to 23.

For about one-third of the sample, one or two of the Pan-STARRS filters have an aperture and PSF magnitude that differ by more than 2.5σ . About 60% of these we identify as possible galaxies below. The majority of the remainder have PSF and aperture magnitude differences that are not large in absolute terms, and it is possible that the uncertainties are slightly underestimated in this Pan-STARRS release.

Sources with Pan-STARRS AB magnitudes $r \lesssim 21$ and $i \lesssim 20.5$ were detected by Gaia, consistent with the $G < 21$ limit of Gaia Data Release 2 (Gaia Collaboration et al. 2018). Of those, about 85% have proper motion measurements (all $\lesssim 30$ mas yr⁻¹). About one-third of the sources with proper motion measurements have a trigonometric parallax measurement that is positive and has an uncertainty smaller than the parallax measurement. Fifteen of the 169 objects found in our searches have a Gaia parallax measurement that is significant. The next release of Gaia data, expected in the third quarter of 2020, will include additional and improved astrometry¹⁰.

6 STAR/GALAXY SEPARATION

Our goal here is to provide as clean a sample as possible of truly point source calibrators, so that, even if imaged at very high resolution, the aperture corresponding to the photometry is unambiguous. We therefore further prune the sample by excluding possible galaxies.

Davies et al. (2018) determined that stars and galaxies can be separated in VISTA data by using a near-infrared colour index. Davies et al. (2018) select for galaxies by applying the colour cut $(H - Ks) - (Y - J) > -0.26$, and verified the selection by visual inspection of objects brighter than $Y = 21.2$. Not all of our sample has a Y -band measurement and we determined the $(H - Ks) - (y_{AB} - J)$ color, replacing the VISTA Y_{Vega} with the Pan-STARRS y_{AB} magni-

¹⁰ <https://www.cosmos.esa.int/web/gaia/release>

tude. Calibrating that index against the VISTA index, we adopt as a stellar indicator $(H - Ks) - (Y - J) < -0.22$ or $(H - Ks) - (y_{AB} - J) < -0.91$.

We also explored the use of the Pan-STARRS PSF and Kron magnitudes, searching for the brighter Kron magnitudes that would be expected if the source was extended (e.g. Chambers et al. 2016, their Figure 19). Chambers et al. (2016) find that stars can be selected by $\text{PSF} - \text{Kron} < 0.05$ magnitude, for magnitudes as faint as ~ 21 .

Figure 1 combines these two indicators, plotting $(H - Ks) - (Y - J)$ and $(H - Ks) - (y_{AB} - J)$ against $\text{PSF} - \text{Kron}$ magnitudes for each of the Pan-STARRS filters. The star/galaxy cuts are shown in the Figure; we excluded as possible galaxies sources which are either too red in one or both of the color indices, or too bright in any of the PSF - Kron colours. The sources that remain are shown in black in Figure 1, and lie to the lower left, or have error bars that would place them in the lower left, of each panel (error bars are omitted from the Figure for clarity). These cuts identified 77 of the 169 sources as possible galaxies, and we omit them from the standard star sample. The Appendix Table B1 lists the possible galaxies together with Pan-STARRS and VISTA-system photometry, and Gaia data where available.

7 EXCLUSION OF MULTIPLE SYSTEMS AND OTHER CONTAMINANTS

We further refine the likely-star sample of 92 objects by excluding sources with atypical colours. These may be multiple systems, or the colours may be compromised in some way. To produce a conservative sample, we reject outliers from colour sequences prescribed by the majority of the sample. Figure 2 shows bluer colours — $g_{AB} - r_{AB}$, $r_{AB} - i_{AB}$, $i_{AB} - z_{AB}$ — and Figure 3 redder colours — $z_{AB} - y_{AB}$, $y_{AB} - J_{Vega}$, $J_{Vega} - H_{Vega}$. We identify 7 sources as outliers; these are shown as open circles in Figures 2 and 3 and listed in Appendix Table C1.

Figures 2 and 3 include color sequences produced by stellar model atmospheres. We used the BT-SETTL models (Allard et al. 2012; Baraffe et al. 2015) and the PARSEC models (Bressan et al. 2012; Girardi et al. 2000), for a range of metallicity as described in the Figure caption. For both model sets the $g - r$ colour deviates significantly from observation for M-type stars; this may be due to some issue common to the model atmospheres or it may be due to errors in the g bandpass adopted by both modelling groups, which could introduce a colour term. The colors and absolute magnitudes (where available), combined with the models, imply that the sample consists of dwarf stars with masses between 0.1 and 1.0 M_{\odot} .

Lastly, for the DXS, VIDEO and WFCAMCAL surveys, where there is no offset between the source table aperture magnitudes and the variability table mean magnitudes (Sections 2, 3), we excluded sources where these values deviated significantly. The earlier selections excluded discrepant sources based on the variability rms, now we exclude sources based on the variability MAD values. We excluded sources where the aperture and mean magnitudes differed by > 0.03 mag and the difference was significant by $> 2.5 \sigma$. Four additional objects were rejected by this criterion and

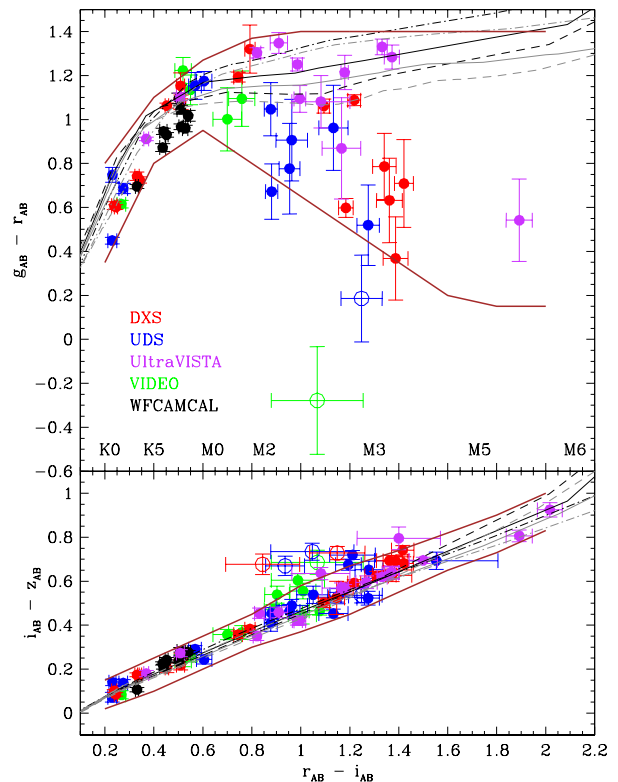


Figure 2. Colours of the likely stellar sources. No reddening correction has been applied. Open circles are objects with one or more colours that deviate from the loci identified by the sample. The thinner lines are model isochrones from the BT-SETTL set (black, Allard et al. (2012); Baraffe et al. (2015)) and the PARSEC set (grey, Bressan et al. (2012); Girardi et al. (2000)). For these sequences, age in Gyr and $[m/H]$ are: 5, 0.0 (solid line); 1.0, +0.3 (dashed line); 10, -0.5 (dash-dot line). The thick brown lines indicate the regions adopted here as defining normal star colours. Two sources are excluded in the top panel, being either too blue in $g_{AB} - r_{AB}$ or in $r_{AB} - i_{AB}$. One of these is also an outlier in the lower panel, along with four other sources that appear too blue in $r_{AB} - i_{AB}$ or too red in $i_{AB} - z_{AB}$. Spectral types along the x axis are from the relationship between $r_{AB} - i_{AB}$ and type given by Covey et al. (2007).

these are listed in Appendix Table C2. All of these rejected sources are at the faint end of the associated survey.

After exclusion of these 11 objects, the final sample consists of 81 stars ranging in spectral type from K2 to M6.

8 FINAL SAMPLE

Table 2 compiles the Pan-STARRS, UKIDSS/VISTA and Gaia data for the final sample of 81 stars. Spectral types are also given; these are estimated from the $r_{AB} - i_{AB}$ color (Covey et al. 2007) where available. Where this color was not available the type was estimated by interpolating the $i_{AB} - z_{AB}$ or $y_{AB} - J_{Vega}$ colors, using stars with all three colors to define the relationships.

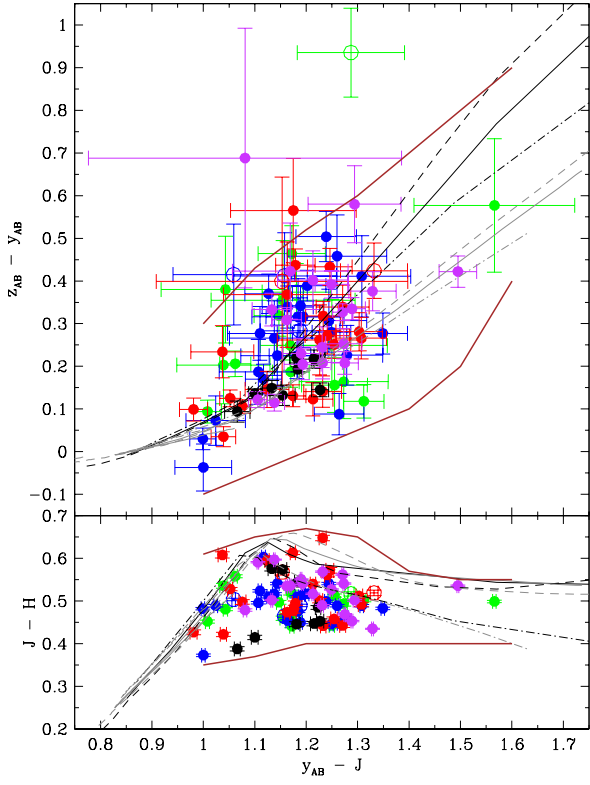


Figure 3. Colours of the likely stellar sources with symbols and lines as in Figure 2. No reddening correction has been applied. In addition to the 6 outliers identified in Figure 2, one additional outlier is identified in the upper panel, as too red in $z_{AB} - y_{AB}$ or too blue in $y_{AB} - J$.

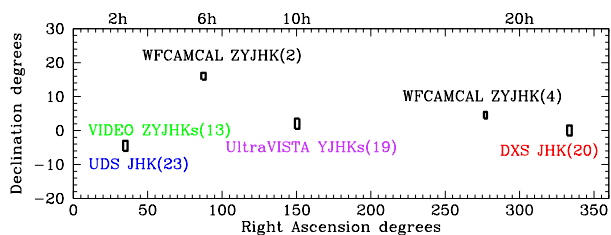


Figure 4. Sky chart showing the location and filter coverage of the final selection of standards. The number of stars at each location is given in parentheses.

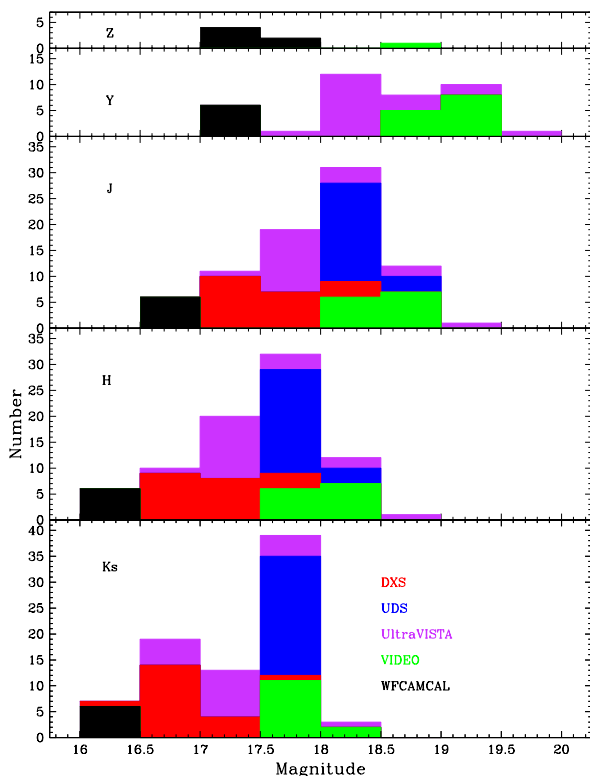


Figure 5. Histogram of magnitude distribution in each filter for each survey, for the final selection of standard stars.

9 CALIBRATION DATA

Tables 3 and 4 list the photometric calibration data for Z and Y, and Tables 5 and 6 list the photometric calibration data for JHK(s), selected from the WFCAM (UKIDSS) and VISTA archives respectively. The transformations between the WFCAM and VISTA systems are given in Section 4. The uncertainties in the magnitudes which have been converted to the VISTA system includes the uncertainty in the transformation.

We only include stars with twenty or more good observations in the variability tables, for each filter, for use as calibrators. Figure 4 illustrates the location on the sky of the new photometric standards, and Figure 5 shows the magnitude distribution for each filter.

The mean magnitude from the variability table, with an uncertainty given by $1.484 \times \text{MagMAD} / \sqrt{n\text{GoodObs}} - 1$, is the fundamental photometric reference for calibration purposes. The photometry presented here has a relative uncer-

tainty of < 0.006 mag. González-Fernández et al. (2018) and Hodgkin et al. (2009) compare the WFCAM and UKIDSS photometric systems, compare each system to the 2MASS system, and compare the WFCAM system to the FS system which is defined by a different camera on UKIRT. The authors also examine the VISTA and WFCAM colours of samples of A0 stars, which by definition are zero. These various comparisons suggest that the VISTA and WFCAM photometric accuracy is $\lesssim 0.02$ mag, which also applies to the sample of stars presented here.

10 CONCLUSIONS

The traditional near-infrared photometric standard stars published by Hawarden et al. (2001) and Leggett et al. (2006) are too bright for efficient observing by current 8- to 10-m class telescopes, and future extremely large 30- to 40-m class telescopes. In order to provide a set of fainter standards for community use, we queried the DXS, UDS, VIDEO and UltraVISTA surveys using the WFCAM and VISTA Science Archives. Non-variable, probable stars were identified with JHK(s) magnitudes between 16 and 19. The initial sample of 169 sources was further refined by excluding 77 objects that may be galaxies, as indicated by red/near-infrared colours or PAN-STARRS Kron magnitudes. Eleven of the remaining sources were excluded due to atypical colours, or discrepant aperture and mean magnitudes from the source and variability tables, respectively. In this way we have produced a sample of 81 non-variable objects with precise photometry, that are likely to be single K and M stars. The new standard stars are distributed equatorially and are accessible from both hemispheres. Table 7 collates the calibration data on the VISTA ZYJHKs photometric system. The table also gives a unique running identification number for convenience — we refer to this as the Very Faint Standard, or VFS, identification number. We also give standard IAU names based on sexagesimal coordinate strings. Finder charts are presented in Appendix D.

Table 3. Standard Stars from WFCAM: ZY

Survey	RA° Decl.°	n Z	Z mean ± mag	Z Aper ± mag	Z rms mag	Z MAD mag	n Y	Y mean ± mag	Y Aper ± mag	Y rms mag	Y MAD mag	ZVISTA ± mag	YVISTA ± mag
CAL	87.7352518 15.8816295	106	17.2521 0.0026	17.2224 0.0149	0.0732	0.0177	121	17.0335 0.0025	17.0391 0.0138	0.0339	0.0183	17.2730 0.0070	17.0544 0.0035
CAL	88.0439399 16.2125856	86	17.4721 0.0053	17.4935 0.0178	0.1718	0.0327	103	17.2724 0.0032	17.2371 0.0154	0.0411	0.0218	17.4837 0.0095	17.2840 0.0044
CAL	276.7225557 4.0587376	133	17.4837 0.0028	17.4682 0.0173	0.0588	0.0218	131	17.2023 0.0030	17.1913 0.0151	0.0544	0.0227	17.4972 0.0081	17.2159 0.0042
CAL	276.8280740 3.9774041	140	17.2483 0.0026	17.2810 0.0155	0.0845	0.0203	138	17.0144 0.0023	17.0237 0.0137	0.0425	0.0181	17.2663 0.0074	17.0325 0.0035
CAL	277.2399424 4.0952285	135	17.5592 0.0038	17.5412 0.0182	0.0638	0.0294	137	17.2465 0.0028	17.2558 0.0160	0.0497	0.0221	17.5724 0.0085	17.2598 0.0041
CAL	277.2699877 4.5221425	135	17.5972 0.0033	17.5926 0.0183	0.0667	0.0257	133	17.3253 0.0028	17.2961 0.0157	0.0560	0.0218	17.6120 0.0081	17.3401 0.0040

Table 4. Standard Stars from VISTA: ZY

Survey	RA ^o Decl. ^o	n Z	Z mean ± mag	Z Aper ± mag	Z rms mag	Z MAD mag	n Y	Y mean ± mag	Y Aper ± mag	Y rms mag	Y MAD mag
VIDEO	35.0542019 -4.4813805						78	19.0018 0.0021	18.9692 0.0098	0.0327	0.0126
VIDEO	35.1152774 -4.9003215						78	19.0704 0.0020	19.0412 0.0088	0.0219	0.0118
VIDEO	35.3795003 -4.6057616						78	19.1025 0.0023	19.0890 0.0089	0.0294	0.0133
VIDEO	35.6598904 -4.6351333						77	18.7513 0.0016	18.7303 0.0052	0.0292	0.0094
VIDEO	35.6610332 -4.5453215						78	19.0260 0.0019	18.9936 0.0075	0.0234	0.0111
VIDEO	35.6959814 -4.5264450						78	19.3279 0.0026	19.2979 0.0105	0.0228	0.0154
VIDEO	35.7281547 -5.2037306						78	19.3492 0.0027	19.3460 0.0112	0.0236	0.0160
VIDEO	35.8660837 -4.1075563						78	19.1724 0.0024	19.1566 0.0106	0.0343	0.0143
VIDEO	35.9623324 -4.2237615						78	18.8035 0.0017	18.7944 0.0088	0.0206	0.0099
VIDEO	35.9681759 -4.2573895						77	18.8680 0.0021	18.8437 0.0288	0.0210	0.0122
VIDEO	35.9729949 -5.2047350						78	18.7733 0.0025	18.8435 0.0290	0.0211	0.0147
VIDEO	36.0194131 -4.8728386						78	19.1804 0.0022	19.1611 0.0144	0.0243	0.0128
VIDEO	36.7075066 -4.5302703	74	18.9232 0.0017	18.8959 0.0072	0.0460	0.0099	75	18.7517 0.0016	18.7244 0.0074	0.0157	0.0092
UVISTA	149.7053794 2.4862294						90	18.3682 0.0013	18.3562 0.0013	0.0122	0.0084
UVISTA	149.7087571 2.7888722						75	18.4555 0.0011	18.4382 0.0020	0.0085	0.0063
UVISTA	149.7234241 2.7511805						75	19.2576 0.0012	19.2364 0.0029	0.0104	0.0071
UVISTA	149.7264829 2.5902461						140	18.3791 0.0013	18.3591 0.0014	0.0133	0.0101
UVISTA	149.7307359 2.7399894						75	18.7503 0.0010	18.7310 0.0023	0.0091	0.0058
UVISTA	149.7313560 2.6928870						143	18.0241 0.0008	18.0070 0.0011	0.0094	0.0066
UVISTA	149.7319650 2.7327131						75	19.8434 0.0022	19.8107 0.0034	0.0181	0.0126
UVISTA	149.7332239 2.7947267						71	18.4389 0.0009	18.4214 0.0020	0.0086	0.0053
UVISTA	149.7355822 2.3205009						140	18.8246 0.0010	18.8101 0.0017	0.0121	0.0077
UVISTA	149.7360512 2.4872598						147	18.0802 0.0008	18.0609 0.0012	0.0109	0.0069
UVISTA	149.7476065 2.7272746						75	19.1804 0.0016	19.1586 0.0025	0.0140	0.0093
UVISTA	149.7564883 2.7279976						75	17.9949 0.0011	17.9755 0.0014	0.0098	0.0063
UVISTA	149.7597522 2.7827541						75	18.4764 0.0012	18.4621 0.0021	0.0097	0.0069
UVISTA	149.7742789 2.6687115						79	18.2324 0.0011	18.2136 0.0013	0.0106	0.0064
UVISTA	149.7772394 2.7783479						75	18.8640 0.0011	18.8447 0.0025	0.0097	0.0065
UVISTA	149.7923194 2.5832843						140	18.1225 0.0012	18.0959 0.0012	0.0123	0.0095
UVISTA	149.8156044 2.7697500						75	18.2690 0.0009	18.2479 0.0018	0.0093	0.0052
UVISTA	149.8172140 2.7717426						75	18.2823 0.0009	18.2632 0.0018	0.0075	0.0054
UVISTA	149.8251519 2.7608222						75	18.3345 0.0010	18.3074 0.0019	0.0102	0.0060

Note: UltraVISTA Y-band source table aperture magnitudes are systematically brighter than the variability table mean magnitudes by ≈ 0.02 mag, due to differences in the aperture correction and zeropoints. All mean magnitudes given in this paper are self-consistent.

Table 5. Standard Stars from WFCAM: *JHK*

Survey	RA ^o Decl. ^o	n <i>J</i>	<i>J</i> mean ± mag	<i>J</i> Aper ± mag	<i>J</i> rms mag	<i>J</i> MAD mag	n <i>H</i>	<i>H</i> mean ± mag	<i>H</i> Aper ± mag	<i>H</i> rms mag	<i>H</i> MAD mag	n <i>K</i>	<i>K</i> mean ± mag	<i>K</i> Aper ± mag	<i>K</i> rms mag	<i>K</i> MAD mag	<i>J</i> VISTA ± mag	<i>H</i> VISTA ± mag	<i>K</i> sVISTA ± mag
UDS	34.0342392	349	18.3349	18.5313	0.0177	0.0108	225	17.8661	18.0749	0.0224	0.0130	513	17.5663	17.7429	0.0267	0.0141	18.3094	17.8626	17.5573
	-5.1728814		0.0009	0.0025				0.0013	0.0022				0.0009	0.0019			0.0020	0.0018	0.0032
UDS	34.0585392	350	18.5195	18.7181	0.0180	0.0108	220	18.0215	18.2202	0.0238	0.0158	522	17.7618	17.9339	0.0286	0.0173	18.4943	18.0184	17.7527
	-5.3530358		0.0009	0.0028				0.0016	0.0024				0.0011	0.0021			0.0020	0.0020	0.0032
UDS	34.0906904	351	18.3316	18.5312	0.0201	0.0117	225	17.8608	18.0636	0.0253	0.0154	516	17.5957	17.7785	0.0273	0.0147	18.3070	17.8586	17.5862
	-5.1871909		0.0009	0.0026				0.0015	0.0023				0.0010	0.0020			0.0020	0.0020	0.0031
UDS	34.1166206	350	18.3820	18.5803	0.0187	0.0119	221	17.8637	18.0607	0.0226	0.0137	522	17.6719	17.8423	0.0295	0.0191	18.3581	17.8624	17.6619
	-5.4330768		0.0009	0.0027				0.0014	0.0023				0.0012	0.0020			0.0020	0.0018	0.0032
UDS	34.1459342	352	18.4145	18.6036	0.0196	0.0125	221	17.8761	18.0775	0.0231	0.0124	524	17.6053	17.7783	0.0264	0.0173	18.3878	17.8711	17.5971
	-5.4192513		0.0010	0.0028				0.0012	0.0023				0.0011	0.0020			0.0021	0.0018	0.0033
UDS	34.1559576	352	18.5141	18.7003	0.0228	0.0129	224	17.9824	18.1923	0.0271	0.0152	516	17.7474	17.9236	0.0304	0.0199	18.4886	17.9790	17.7385
	-5.1864870		0.0010	0.0029				0.0015	0.0025				0.0013	0.0022			0.0021	0.0020	0.0033
UDS	34.1991747	353	18.3649	18.5502	0.0199	0.0138	221	17.8259	18.0177	0.0248	0.0143	524	17.5907	17.7792	0.0254	0.0170	18.3392	17.8223	17.5819
	-4.9476391		0.0011	0.0028				0.0011	0.0022				0.0011	0.0020			0.0021	0.0019	0.0033
UDS	34.2232606	386	18.5385	18.7258	0.0227	0.0139	257	17.9753	18.1769	0.0291	0.0184	604	17.7418	17.9272	0.0344	0.0215	18.5122	17.9708	17.7333
	-4.7491396		0.0010	0.0028				0.0017	0.0023				0.0013	0.0022			0.0022	0.0021	0.0034
UDS	34.2308454	351	18.3830	18.5733	0.0206	0.0130	222	17.9104	18.1110	0.0315	0.0162	535	17.6311	17.8114	0.0264	0.0186	18.3580	17.9076	17.6218
	-5.3911233		0.0010	0.0023				0.0016	0.0021				0.0012	0.0019			0.0021	0.0020	0.0032
UDS	34.3103343	348	18.5864	18.7776	0.0259	0.0143	227	18.0813	18.2905	0.0252	0.0132	533	17.7619	17.9373	0.0285	0.0169	18.5593	18.0758	17.7539
	-5.4172864		0.0011	0.0030				0.0013	0.0026				0.0011	0.0021			0.0022	0.0018	0.0034
UDS	34.3240632	345	18.5039	18.6955	0.0211	0.0149	227	17.9932	18.2027	0.0273	0.0154	530	17.6775	17.8517	0.0298	0.0174	18.4768	17.9876	17.6696
	-5.4334966		0.0012	0.0029				0.0015	0.0024				0.0011	0.0020			0.0023	0.0020	0.0034
UDS	34.3475622	345	18.3321	18.5255	0.0178	0.0110	227	17.8488	18.0557	0.0205	0.0128	531	17.5860	17.7628	0.0243	0.0150	18.3072	17.8462	17.5767
	-5.4844981		0.0009	0.0026				0.0013	0.0022				0.0010	0.0019			0.0020	0.0018	0.0032
UDS	34.3750969	345	18.5027	18.6924	0.0183	0.0109	227	17.9403	18.1475	0.0221	0.0140	531	17.6520	17.8285	0.0240	0.0149	18.4748	17.9338	17.6445
	-5.4848715		0.0009	0.0028				0.0014	0.0023				0.0010	0.0020			0.0022	0.0019	0.0034
UDS	34.4389254	339	18.3909	18.5846	0.0219	0.0131	222	17.8585	18.0665	0.0250	0.0155	517	17.6173	17.8000	0.0284	0.0192	18.3653	17.8549	17.6085
	-5.4868910		0.0011	0.0027				0.0015	0.0022				0.0013	0.0020			0.0021	0.0020	0.0033
UDS	34.5319836	439	18.4015	18.5871	0.0195	0.0119	270	17.8547	18.0507	0.0263	0.0148	627	17.6405	17.8118	0.0321	0.0213	18.3762	17.8516	17.6315
	-5.1015107		0.0008	0.0022				0.0013	0.0019				0.0013	0.0018			0.0020	0.0018	0.0033
UDS	34.6700469	374	18.3749	18.5585	0.0244	0.0165	247	17.8552	18.0493	0.0668	0.0160	576	17.5183	17.7034	0.0378	0.0265	18.3469	17.8485	17.5109
	-5.0787756		0.0013	0.0024				0.0015	0.0020				0.0016	0.0019			0.0024	0.0020	0.0036
UDS	34.6776197	404	18.4691	18.6542	0.0231	0.0140	244	17.9327	18.1342	0.0330	0.0149	594	17.6670	17.8461	0.0447	0.0257	18.4426	17.9281	17.6586
	-4.9671258		0.0010	0.0023				0.0014	0.0020				0.0016	0.0019			0.0022	0.0019	0.0035
UDS	34.7079081	347	18.1715	18.3579	0.0152	0.0095	229	17.6592	17.8669	0.0208	0.0123	533	17.5672	17.7433	0.0286	0.0166	18.1506	17.6618	17.5555
	-4.9039390		0.0008	0.0022				0.0012	0.0018				0.0011	0.0018			0.0017	0.0017	0.0029
UDS	34.7425103	345	18.2942	18.4874	0.0200	0.0129	229	17.7883	17.9945	0.0249	0.0142	529	17.7077	17.8798	0.0293	0.0193	18.2738	17.7916	17.6957
	-5.4781043		0.0010	0.0028				0.0014	0.0023				0.0012	0.0022			0.0019	0.0018	0.0029
UDS	34.7745424	371	18.4765	18.6584	0.0215	0.0125	260	17.9661	18.1642	0.0264	0.0162	595	17.6479	17.8183	0.0336	0.0210	18.4493	17.9604	17.6400
	-4.8889668		0.0010	0.0024				0.0015	0.0021				0.0013	0.0019			0.0022	0.0020	0.0034
UDS	34.8172698	354	18.6678	18.8510	0.0221	0.0148	220	18.1916	18.3840	0.0243	0.0143	521	17.9121	18.0983	0.0347	0.0194	18.6426	18.1886	17.9029
	-4.7942724		0.0012	0.0029				0.0014	0.0027				0.0013	0.0024			0.0022	0.0019	0.0033
UDS	34.8182276	404	18.5294	18.7202	0.0220	0.0122	249	17.9046	18.1129	0.0277	0.0150	619	17.7394	17.9188	0.0338	0.0221	18.5033	17.9004	17.7308
	-5.1062739		0.0009	0.0025				0.0014	0.0020				0.0013	0.0020			0.0021	0.0019	0.0034
UDS	34.8710949	366	18.3653	18.5585	0.0178	0.0112	228	17.9672	18.1734	0.0259	0.0157	536	17.8937	18.0786	0.0387	0.0240	18.3481	17.9747	17.8797
	-5.1154861		0.0009	0.0025				0.0015	0.0023				0.0015	0.0023			0.0016	0.0019	0.0029
CAL	87.7352518	136	16.6289	16.6552	0.0591	0.0219	132	16.2164	16.1917	0.0522	0.0301	136	16.1131	16.1481	0.0639	0.0424	16.6104	16.2224	16.0999
	15.8816295		0.0028	0.0160				0.0039	0.0139				0.0054	0.0229			0.0031	0.0041	0.0060
CAL	88.0439399	130	16.7948	16.7686	0.0543	0.0338	125	16.1988	16.1922	0.0559	0.0251	133	16.0276	16.0285	0.0613	0.0313	16.7693	16.1954	16.0186
	16.2125856		0.0044	0.0170				0.0033	0.0137				0.0040	0.0214			0.0048	0.0036	0.0051
CAL	276.7225557	156	16.7231	16.7228	0.0678	0.0261	157	16.1566	16.1678	0.0612	0.0271	167	16.0093	16.0034	0.0665	0.0370	16.6992	16.1551	15.9994
	4.0587376		0.0031	0.0174				0.0032	0.0151				0.0043	0.0252			0.0036	0.0034	0.0052
CAL	276.8280740	158	16.6085	16.6102	0.0485	0.0270	157	16.1697	16.1597	0.0612	0.0255	169	16.0157	16.0139	0.0750	0.0381	16.5879	16.1728	16.0038
	3.9774041		0.0032	0.0162				0.0030	0.0149				0.0044	0.0254			0.0036	0.0033	0.0051
CAL	277.2399424	156	16.7699	16.8010	0.0727	0.0270	154	16.3020	16.2767	0.0543	0.0294	168	16.0474	16.0938	0.0716	0.0369	16.7456	16.3002	16.0376
	4.0952285		0.0032	0.0187				0.0035	0.0169				0.0042	0.0263			0.0037	0.0037	0.0052
CAL	277.2699877	157	16.8103	16.8261	0.0741	0.0277	156	16.3346	16.3425	0.0621	0.0291	167	16.1284	16.1660	0.0715	0.0422	16.7872	16.3344	16.1180
	4.5221425		0.0033	0.0181				0.0035	0.0171				0.0049	0.0262			0.0037	0.0037	0.0056

Note: UDS aperture magnitudes are not aperture corrected and are systematically fainter than the mean magnitudes by ≈ 0.2 mag.

Table 5 – continued Standard Stars from WFCAM: JHK

Survey	RA ^o Decl. ^o	n	J	J mean ± mag	J Aper ± mag	J rms mag	J MAD mag	n	H	H mean ± mag	H Aper ± mag	H rms mag	H MAD mag	n	K	K mean ± mag	K Aper ± mag	K rms mag	K MAD mag	J _{VISTA} ± mag	H _{VISTA} ± mag	K _{S_{VISTA}} ± mag
DXS	333.0711763	26	17.3850	17.3946	0.0128	0.0067								22	16.5895	16.5916	0.0227	0.0105	17.3587	16.8191	16.5811	
	0.8303505		0.0020	0.0071											0.0034	0.0068			0.0027	0.0029	0.0046	
DXS	333.0715557	26	18.1809	18.1990	0.0202	0.0099								22	17.4019	17.4092	0.0224	0.0138	18.1551	17.6539	17.3931	
	0.9162355		0.0029	0.0106											0.0045	0.0115			0.0035	0.0036	0.0054	
DXS	333.0718253	26	18.2282	18.2278	0.0212	0.0125								22	17.4554	17.4472	0.0250	0.0155	18.2026	17.5949	17.4465	
	1.1889522		0.0037	0.0109											0.0050	0.0129			0.0042	0.0055	0.0059	
DXS	333.2839533	24	17.8141	17.8167	0.0133	0.0075								27	17.0182	17.0135	0.0258	0.0126	17.7879	17.2757	17.0097	
	-0.4105822		0.0023	0.0089											0.0037	0.0085			0.0030	0.0050	0.0048	
DXS	333.2928434	24	17.4314	17.4294	0.0159	0.0069	29	16.9668	16.9427	0.0145	0.0111	24	16.7012	16.7006	0.0245	0.0124	17.4070	16.9648	16.6916			
	0.7343005		0.0021	0.0072				0.0031	0.0059				0.0038	0.0074			0.0028	0.0033	0.0048			
DXS	333.3028790	24	17.5811	17.5772	0.0156	0.0095	29	17.1164	17.1209	0.0175	0.0124	24	16.8181	16.8164	0.0194	0.0145	17.5557	17.1132	16.8090			
	0.7544734		0.0029	0.0077				0.0035	0.0062				0.0045	0.0077			0.0035	0.0037	0.0054			
DXS	333.3594622	24	18.3253	18.3266	0.0170	0.0095	29	17.8289	17.8372	0.0277	0.0114	24	17.5693	17.5466	0.0278	0.0156	18.3002	17.8259	17.5602			
	0.7512320		0.0029	0.0114				0.0032	0.0095				0.0048	0.0123			0.0034	0.0034	0.0057			
DXS	333.3824122	24	17.8349	17.8492	0.0114	0.0064	29	17.3366	17.3456	0.0197	0.0122	24	17.0058	17.0084	0.0220	0.0115	17.8077	17.3309	16.9979			
	0.7424491		0.0020	0.0089				0.0034	0.0071				0.0036	0.0087			0.0028	0.0037	0.0048			
DXS	333.4515020	24	17.7055	17.6906	0.0147	0.0131	29	17.2250	17.2250	0.0161	0.0104	24	16.9639	16.9546	0.0193	0.0126	17.6807	17.2226	16.9545			
	0.7278254		0.0040	0.0082				0.0029	0.0070				0.0039	0.0086			0.0044	0.0032	0.0049			
DXS	333.4987510	24	17.9579	17.9683	0.0163	0.0092	29	17.4404	17.4481	0.0223	0.0146	24	17.1523	17.1722	0.0199	0.0134	17.9313	17.4356	17.1440			
	0.7349581		0.0029	0.0094				0.0041	0.0075				0.0042	0.0096			0.0034	0.0043	0.0052			
DXS	333.7094552	25	17.2900	17.2783	0.0111	0.0052	27	16.6727	16.6579	0.0205	0.0103	22	16.5390	16.5553	0.0227	0.0175	17.2650	16.6699	16.5297			
	0.5245924		0.0016	0.0066				0.0030	0.0050				0.0057	0.0066			0.0024	0.0032	0.0064			
DXS	333.9366041	24	17.3359	17.3307	0.0087	0.0045								24	16.5021	16.5124	0.0240	0.0126	17.3086	16.6614	16.4942	
	-0.9471891		0.0014	0.0070									0.0039	0.0063			0.0024	0.0058	0.0050			
DXS	334.6493784	33	17.8736	17.8719	0.0140	0.0128	20	17.2809	17.2940	0.0240	0.0154	44	16.9888	16.9910	0.0264	0.0169	17.8448	17.2731	16.9818			
	1.3819891		0.0033	0.0087				0.0053	0.0077				0.0038	0.0086			0.0039	0.0054	0.0051			
DXS	334.8182190	32	17.6887	17.6897	0.0187	0.0107								34	16.8830	16.8723	0.0267	0.0168	17.6622	17.1697	16.8747	
	0.3928450		0.0029	0.0087									0.0043	0.0083			0.0034	0.0044	0.0054			
DXS	334.9251383	31	17.4395	17.4246	0.0122	0.0093	21	16.8880	16.8930	0.0102	0.0033	34	16.7863	16.7858	0.0329	0.0148	17.4172	16.8889	16.7754			
	0.7274321		0.0025	0.0074				0.0011	0.0061				0.0038	0.0078			0.0030	0.0016	0.0047			
DXS	335.0303119	29	17.4586	17.4514	0.0215	0.0135	22	17.0071	17.0150	0.0140	0.0103	30	16.9359	16.9255	0.0234	0.0150	17.4399	17.0128	16.9227			
	0.4454373		0.0038	0.0076				0.0033	0.0067				0.0041	0.0086			0.0040	0.0035	0.0049			
DXS	335.4746997	45	17.3876	17.3823	0.0200	0.0111	33	16.8051	16.8104	0.0159	0.0119	46	16.5574	16.5396	0.0301	0.0170	17.3604	16.7993	16.5495			
	0.5091841		0.0025	0.0072				0.0031	0.0054				0.0038	0.0067			0.0031	0.0034	0.0049			
DXS	335.5234567	31	17.1940	17.1661	0.0169	0.0117	26	16.6729	16.6621	0.0166	0.0116	32	16.5534	16.5204	0.0242	0.0165	17.1721	16.6742	16.5423			
	0.2874459		0.0032	0.0066				0.0034	0.0051				0.0044	0.0068			0.0036	0.0036	0.0052			
DXS	335.5823067	28	17.3988	17.4093	0.0155	0.0086								33	16.6114	16.6016	0.0201	0.0106	17.3728	16.7596	16.6027	
	-0.1444080		0.0024	0.0074									0.0028	0.0070			0.0031	0.0034	0.0042			
DXS	335.6150576	31	17.3103	17.3109	0.0124	0.0083	26	16.8637	16.8537	0.0144	0.0114	32	16.7785	16.7719	0.0269	0.0180	17.2914	16.8690	16.7655			
	0.5091194		0.0023	0.0070				0.0034	0.0056				0.0048	0.0078			0.0027	0.0036	0.0054			

Table 6. Standard Stars from VISTA: *JHKs*

Survey	RA ^o Decl. ^o	n	<i>J</i> mean ± mag	<i>J</i> Aper ± mag	<i>J</i> rms mag	<i>J</i> MAD mag	n	<i>H</i> mean ± mag	<i>H</i> Aper ± mag	<i>H</i> rms mag	<i>H</i> MAD mag	n	<i>Ks</i> mean ± mag	<i>Ks</i> Aper ± mag	<i>Ks</i> rms mag	<i>Ks</i> MAD mag
VIDEO	35.0542019	39	18.5465	18.5352	0.0178	0.0117	40	18.0267	18.0154	0.0331	0.0198	48	17.8310	17.8200	0.0394	0.0199
	-4.4813805		0.0028	0.0093				0.0047	0.0087				0.0043	0.0097		
VIDEO	35.1152774	39	18.5271	18.5256	0.0174	0.0085	40	18.0857	18.0768	0.0243	0.0134	48	17.8255	17.8019	0.0366	0.0225
	-4.9003215		0.0021	0.0081				0.0032	0.0080				0.0049	0.0088		
VIDEO	35.3795003	39	18.6101	18.5996	0.0138	0.0096	40	18.1286	18.1186	0.0174	0.0120	48	17.9108	17.8928	0.0369	0.0225
	-4.6057616		0.0023	0.0081				0.0028	0.0077				0.0049	0.0085		
VIDEO	35.6598904	39	18.3307	18.3223	0.0343	0.0083	40	17.7733	17.7600	0.0237	0.0126	48	17.6104	17.5946	0.0293	0.0146
	-4.635133		0.0020	0.0050				0.0030	0.0047				0.0032	0.0054		
VIDEO	35.6610332	39	18.5364	18.5202	0.0155	0.0087	40	18.0755	18.0640	0.0200	0.0104	48	17.8501	17.8392	0.0403	0.0182
	-4.5453215		0.0021	0.0070				0.0025	0.0070				0.0039	0.0076		
VIDEO	35.6959814	39	18.9173	18.9030	0.0226	0.0148	40	18.3808	18.3622	0.0287	0.0180	48	18.1880	18.1696	0.0400	0.0228
	-4.5264450		0.0036	0.0101				0.0043	0.0097				0.0049	0.0107		
VIDEO	35.7281547	39	18.8672	18.8681	0.0221	0.0121	40	18.4067	18.4025	0.0310	0.0172	48	18.1372	18.1443	0.0398	0.0244
	-5.2037306		0.0029	0.0101				0.0041	0.0098				0.0053	0.0105		
VIDEO	35.8660837	39	18.6624	18.6644	0.0170	0.0100	40	18.1648	18.1651	0.0240	0.0175	48	17.9286	17.9385	0.0383	0.0229
	-4.1075563		0.0024	0.0098				0.0042	0.0094				0.0050	0.0104		
VIDEO	35.9623324	39	18.3172	18.3222	0.0195	0.0089	40	17.8155	17.8129	0.0239	0.0142	48	17.5798	17.5857	0.0345	0.0208
	-4.2237615		0.0021	0.0080				0.0034	0.0078				0.0045	0.0086		
VIDEO	35.9681759	39	18.3799	18.3917	0.0163	0.0116	40	17.9367	17.9951	0.0207	0.0116	48	17.7016	17.7283	0.0354	0.0193
	-4.2573895		0.0028	0.0247				0.0028	0.0325				0.0042	0.0279		
VIDEO	35.9729949	39	18.2901	18.3199	0.0252	0.0092	40	17.7774	17.7690	0.0205	0.0120	48	17.5529	17.6046	0.0367	0.0182
	-5.2047350		0.0022	0.0583				0.0028	0.0551				0.0039	0.0430		
VIDEO	36.0194131	39	18.4466	18.4416	0.0169	0.0098	40	17.9480	17.9333	0.0218	0.0089	48	17.6283	17.6006	0.0367	0.0203
	-4.8728386		0.0024	0.0119				0.0021	0.0121				0.0044	0.0116		
VIDEO	36.7075066	38	18.4144	18.3932	0.0273	0.0091	40	17.9624	17.9428	0.0301	0.0142	50	17.8677	17.8408	0.0336	0.0189
	-4.5302703		0.0022	0.0073				0.0034	0.0075				0.0040	0.0082		
UVISTA	149.7053794	131	17.8524	17.8119	0.0095	0.0066	232	17.3109	17.3465	0.0362	0.0105	199	17.0759	17.0883	0.0175	0.0093
	2.4862294		0.0009	0.0012				0.0010	0.0012				0.0010	0.0012		
UVISTA	149.7087571	80	17.9656	17.9106	0.0086	0.0047	123	17.4313	17.4534	0.0155	0.0092	101	17.2116	17.2032	0.0182	0.0121
	2.7888722		0.0008	0.0019				0.0012	0.0018				0.0018	0.0019		
UVISTA	149.7234241	80	18.6410	18.5871	0.0117	0.0071	123	18.1390	18.1468	0.0238	0.0139	101	17.8376	17.8220	0.0237	0.0143
	2.7511805		0.0012	0.0027				0.0019	0.0023				0.0021	0.0024		
UVISTA	149.7264829	150	17.8180	17.7721	0.0094	0.0057	236	17.2913	17.3231	0.0750	0.0110	203	17.0327	17.0421	0.0169	0.0115
	2.5902461		0.0007	0.0012				0.0011	0.0012				0.0012	0.0012		
UVISTA	149.7307359	80	18.1943	18.1414	0.0083	0.0045	123	17.6766	17.7059	0.0194	0.0100	101	17.4237	17.4190	0.0194	0.0129
	2.7399894		0.0008	0.0021				0.0013	0.0020				0.0019	0.0020		
UVISTA	149.7313560	158	17.5590	17.5094	0.0075	0.0047	252	17.0082	17.0394	0.0394	0.0100	206	16.7933	16.8107	0.0159	0.0084
	2.6928870		0.0006	0.0011				0.0009	0.0011				0.0009	0.0011		
UVISTA	149.7319650	80	19.2441	19.1790	0.0188	0.0118	123	18.7651	18.7666	0.0308	0.0186	101	18.4652	18.4630	0.0324	0.0225
	2.7327131		0.0020	0.0031				0.0025	0.0027				0.0033	0.0031		
UVISTA	149.7332239	78	17.8730	17.8189	0.0084	0.0048	120	17.4382	17.4644	0.0167	0.0095	97	17.1655	17.1668	0.0183	0.0106
	2.7947267		0.0008	0.0018				0.0013	0.0018				0.0016	0.0019		
UVISTA	149.7355822	150	18.3514	18.3066	0.0107	0.0055	236	17.7820	17.7993	0.0887	0.0123	203	17.5625	17.5589	0.0215	0.0130
	2.3205009		0.0007	0.0015				0.0012	0.0015				0.0014	0.0015		
UVISTA	149.7360512	152	17.6720	17.6253	0.0087	0.0051	232	17.0809	17.1141	0.0622	0.0093	199	16.9594	16.9764	0.0186	0.0092
	2.4872598		0.0006	0.0011				0.0009	0.0011				0.0010	0.0012		
UVISTA	149.7476065	80	18.6534	18.6047	0.0125	0.0087	123	18.1630	18.1692	0.0262	0.0129	101	17.9131	17.9004	0.0306	0.0182
	2.7272746		0.0014	0.0023				0.0017	0.0021				0.0027	0.0022		
UVISTA	149.7564883	80	17.4583	17.4066	0.0078	0.0048	123	16.8964	16.9283	0.0164	0.0073	101	16.6443	16.6641	0.0150	0.0078
	2.7279976		0.0008	0.0013				0.0010	0.0012				0.0012	0.0013		
UVISTA	149.7597522	80	17.8232	17.7737	0.0084	0.0053	123	17.2872	17.3208	0.0191	0.0106	101	16.9664	16.9830	0.0159	0.0100
	2.7827541		0.0009	0.0018				0.0014	0.0017				0.0015	0.0018		
UVISTA	149.7742789	104	17.8107	17.7615	0.0100	0.0056	251	17.2140	17.2393	0.0799	0.0111	206	17.0529	17.0630	0.0172	0.0093
	2.6687115		0.0008	0.0013				0.0010	0.0012				0.0010	0.0013		
UVISTA	149.7772394	80	18.3290	18.2735	0.0110	0.0069	123	17.7934	17.8162	0.0248	0.0105	101	17.5463	17.5351	0.0218	0.0121
	2.7783479		0.0011	0.0023				0.0014	0.0021				0.0018	0.0021		
UVISTA	149.7923194	150	17.5830	17.5310	0.0076	0.0046	237	17.1304	17.1662	0.0826	0.0114	203	16.8712	16.8883	0.0161	0.0096
	2.5832843		0.0006	0.0011				0.0011	0.0011				0.0010	0.0011		
UVISTA	149.8156044	80	17.7772	17.7230	0.0097	0.0057	123	17.2745	17.3082	0.0174	0.0074	101	17.0546	17.0646	0.0184	0.0090
	2.7697500		0.0010	0.0018				0.0010	0.0017				0.0013	0.0018		
UVISTA	149.8172140	80	17.8016	17.7487	0.0074	0.0049	123	17.2609	17.2904	0.0202	0.0098	101	17.0372	17.0491	0.0165	0.0096
	2.7717426		0.0008	0.0018				0.0013	0.0017				0.0014	0.0018		
UVISTA	149.8251519	80	17.8417	17.7810	0.0074	0.0041	123	17.3732	17.3980	0.0165	0.0089	101	17.1457	17.1466	0.0187	0.0097
	2.7608222		0.0007	0.0018				0.0012	0.0017				0.0014	0.0018		

Note: UltraVISTA source table aperture magnitudes are systematically brighter than the variability table mean magnitudes by ≈ 0.05 mag at *J*, and fainter by ≈ 0.02 mag at *H*, due to differences in the aperture correction and zeropoints. All mean magnitudes given in this paper are self-consistent.

ACKNOWLEDGEMENTS

The authors gratefully acknowledge the work of Mike Irwin and the Cambridge Astronomical Survey Unit (CASU) along with Mike Read and the Edinburgh Wide Field Astronomy Unit (WFAU) for their tireless work in generating and serving the wide field infrared public surveys from UKIRT and VISTA. We also acknowledge the selfless work by the respective public survey leads: Alastair Edge (DXS), Omar Almaini (UDS), Marijn Franx and Jim Dunlop (UltraVISTA) and Matt Jarvis (VIDEO).

The Pan-STARRS Survey and science archive have been made possible through contributions by the Institute for Astronomy, the University of Hawaii, the Pan-STARRS Project Office, the Max-Planck Society and its participating institutes, the Max Planck Institute for Astronomy, Heidelberg and the Max Planck Institute for Extraterrestrial Physics, Garching, The Johns Hopkins University, Durham University, the University of Edinburgh, the Queen's University Belfast, the Harvard-Smithsonian Center for Astrophysics, the Las Cumbres Observatory Global Telescope Network Incorporated, the National Central University of Taiwan, the Space Telescope Science Institute, the National Aeronautics and Space Administration under Grant No. NNX08AR22G issued through the Planetary Science Division of the NASA Science Mission Directorate, the National Science Foundation Grant No. AST-1238877, the University of Maryland, Eotvos Lorand University (ELTE), the Los Alamos National Laboratory, and the Gordon and Betty Moore Foundation.

This work presents results from the European Space Agency (ESA) space mission Gaia. Gaia data are being processed by the Gaia Data Processing and Analysis Consortium (DPAC). Funding for the DPAC is provided by national institutions, in particular the institutions participating in the Gaia MultiLateral Agreement (MLA). The Gaia mission website is <https://www.cosmos.esa.int/gaia>. The Gaia archive website is <https://archives.esac.esa.int/gaia>.

REFERENCES

- Allard F., Homeier D., Freytag B., 2012, *Philosophical Transactions of the Royal Society of London Series A*, 370, 2765
- Baraffe I., Homeier D., Allard F., Chabrier G., 2015, *A&A*, 577, A42
- Bertin E., Arnouts S., 1996, *A&AS*, 117, 393
- Bertin E., Mellier Y., Radovich M., Missonnier G., Didelon P., Morin B., 2002, The TERAPIX Pipeline. p. 228
- Bressan A., Marigo P., Girardi L., Salasnich B., Dal Cero C., Rubele S., Nanni A., 2012, *MNRAS*, 427, 127
- Chambers K. C., et al., 2016, arXiv e-prints, p. arXiv:1612.05560
- Covey K. R., et al., 2007, *AJ*, 134, 2398
- Cross N. J. G., Collins R. S., Hambly N. C., Blake R. P., Read M. A., Sutorius E. T. W., Mann R. G., Williams P. M., 2009, *MNRAS*, 399, 1730
- Cross N. J. G., et al., 2012, *A&A*, 548, A119
- Davies L. J. M., et al., 2018, *MNRAS*, 480, 768
- Dye S., et al., 2018, *MNRAS*, 473, 5113
- Ferreira Lopes C. E., Dékány I., Catelan M., Cross N. J. G., Angeloni R., Leão I. C., De Medeiros J. R., 2015, *A&A*, 573, A100
- Finkbeiner D. P., et al., 2016, *ApJ*, 822, 66
- Gaia Collaboration et al., 2016, *A&A*, 595, A1
- Gaia Collaboration et al., 2018, *A&A*, 616, A1
- Girardi L., Bressan A., Bertelli G., Chiosi C., 2000, *A&AS*, 141, 371
- González-Fernández C., et al., 2018, *MNRAS*, 474, 5459
- Hambly N. C., et al., 2008, *MNRAS*, 384, 637
- Hawarden T. G., Leggett S. K., Letawsky M. B., Ballantyne D. R., Casali M. M., 2001, *MNRAS*, 325, 563
- Hodapp K. W., et al., 2018, in *Ground-based and Airborne Telescopes VII*. p. 107002Z, doi:10.1117/12.2311923
- Hodgkin S. T., Irwin M. J., Hewett P. C., Warren S. J., 2009, *MNRAS*, 394, 675
- Irwin M. J., et al., 2004, in Quinn P. J., Bridger A., eds, *Society of Photo-Optical Instrumentation Engineers (SPIE) Conference Series Vol. 5493, Optimizing Scientific Return for Astronomy through Information Technologies*. pp 411–422, doi:10.1117/12.551449
- Jarvis M. J., et al., 2013, *MNRAS*, 428, 1281
- Lawrence A., et al., 2007, *MNRAS*, 379, 1599
- Leggett S. K., et al., 2006, *MNRAS*, 373, 781
- Liske J., Lemon D. J., Driver S. P., Cross N. J. G., Couch W. J., 2003, *MNRAS*, 344, 307
- McCracken H. J., et al., 2012, *A&A*, 544, A156
- Padmanabhan N., et al., 2008, *ApJ*, 674, 1217
- Skrutskie M. F., et al., 2006, *AJ*, 131, 1163
- Sutherland W., et al., 2015, *A&A*, 575, A25
- Tokunaga A. T., Simons D. A., Vacca W. D., 2002, *PASP*, 114, 180
- Tonry J. L., et al., 2012, *ApJ*, 750, 99
- Warren S. J., et al., 2007, *Monthly Notices of the Royal Astronomical Society*, 375, 213
- York D. G., et al., 2000, *AJ*, 120, 1579

Table 7. Standard Stars with VISTA-System *ZYJHKs*. The first and second columns give a unique running number for convenience (VFS = ‘Very Faint Standard’) and a formal IAU designation for each star.

VFS	IAU name	RA ^o _{n Z} Decl. ^o	Z _{n Y} ± mag	Y _{n J} ± mag	J _{n H} ± mag	H _{n Ks} ± mag	K _s ± mag					
1	UUDS J021608.22-051022.4	34.0342392 -5.1728814		349	18.3094 0.0020	225	17.8626 0.0018	513	17.5573 0.0032			
2	UUDS J021614.05-052110.9	34.0585392 -5.3530358		350	18.4943 0.0020	220	18.0184 0.0020	522	17.7527 0.0032			
3	UUDS J021621.77-051113.9	34.0906904 -5.1871909		351	18.3070 0.0020	225	17.8586 0.0020	516	17.5862 0.0031			
4	UUDS J021627.99-052559.1	34.1166206 -5.4330768		350	18.3581 0.0020	221	17.8624 0.0018	522	17.6619 0.0032			
5	UUDS J021635.02-052509.3	34.1459342 -5.4192513		352	18.3878 0.0021	221	17.8711 0.0018	524	17.5971 0.0033			
6	UUDS J021637.43-051111.4	34.1559576 -5.1864870		352	18.4886 0.0021	224	17.9790 0.0020	516	17.7385 0.0033			
7	UUDS J021647.80-045651.5	34.1991747 -4.9476391		353	18.3392 0.0021	221	17.8223 0.0019	524	17.5819 0.0033			
8	UUDS J021653.58-044456.9	34.2232606 -4.7491396		386	18.5122 0.0022	257	17.9708 0.0021	604	17.7333 0.0034			
9	UUDS J021655.40-052328.0	34.2308454 -5.3911233		351	18.3580 0.0021	222	17.9076 0.0020	535	17.6218 0.0032			
10	UUDS J021714.48-052502.2	34.3103343 -5.4172864		348	18.5593 0.0022	227	18.0758 0.0018	533	17.7539 0.0034			
11	UUDS J021717.78-052600.6	34.3240632 -5.4334966		345	18.4768 0.0023	227	17.9876 0.0020	530	17.6696 0.0034			
12	UUDS J021723.41-052904.2	34.3475622 -5.4844981		345	18.3072 0.0020	227	17.8462 0.0018	531	17.5767 0.0032			
13	UUDS J021730.02-052905.5	34.3750969 -5.4848715		345	18.4748 0.0022	227	17.9338 0.0019	531	17.6445 0.0034			
14	UUDS J021745.34-052912.8	34.4389254 -5.4868910		339	18.3653 0.0021	222	17.8549 0.0020	517	17.6085 0.0033			
15	UUDS J021807.68-050605.4	34.5319836 -5.1015107		439	18.3762 0.0020	270	17.8516 0.0018	627	17.6315 0.0033			
16	UUDS J021840.81-050443.6	34.6700469 -5.0787756		374	18.3469 0.0024	247	17.8485 0.0020	576	17.5109 0.0036			
17	UUDS J021842.63-045801.7	34.6776197 -4.9671258		404	18.4426 0.0022	244	17.9281 0.0019	594	17.6586 0.0035			
18	UUDS J021849.90-045414.2	34.7079081 -4.9039390		347	18.1506 0.0017	229	17.6618 0.0017	533	17.5555 0.0029			
19	UUDS J021858.20-052841.2	34.7425103 -5.4781043		345	18.2738 0.0019	229	17.7916 0.0018	529	17.6957 0.0029			
20	UUDS J021905.89-045320.3	34.7745424 -4.8889668		371	18.4493 0.0022	260	17.9604 0.0020	595	17.6400 0.0034			
21	UUDS J021916.14-044739.4	34.8172698 -4.7942724		354	18.6426 0.0022	220	18.1886 0.0019	521	17.9029 0.0033			
22	UUDS J021916.37-050622.6	34.8182276 -5.1062739		404	18.5033 0.0021	249	17.9004 0.0019	619	17.7308 0.0034			
23	UUDS J021929.06-050655.7	34.8710949 -5.1154861		366	18.3481 0.0016	228	17.9747 0.0019	536	17.8797 0.0029			
24	VIDEO J022013.01-042853.0	35.0542019 -4.4813805	78	19.0018 0.0021	39	18.5465 0.0028	40	18.0267 0.0047	48	17.8310 0.0043		
25	VIDEO J022027.67-045401.2	35.1152774 -4.9003215	78	19.0704 0.0020	39	18.5271 0.0021	40	18.0857 0.0032	48	17.8255 0.0049		
26	VIDEO J022131.08-043620.7	35.3795003 -4.6057616	78	19.1025 0.0023	39	18.6101 0.0023	40	18.1286 0.0028	48	17.9108 0.0049		
27	VIDEO J022238.37-043806.5	35.6598904 -4.6351333	77	18.7513 0.0016	39	18.3307 0.0020	40	17.7733 0.0030	48	17.6104 0.0032		
28	VIDEO J022238.65-043243.2	35.6610332 -4.5453215	78	19.0260 0.0019	39	18.5364 0.0021	40	18.0755 0.0025	48	17.8501 0.0039		
29	VIDEO J022247.04-043135.2	35.6959814 -4.5264450	78	19.3279 0.0026	39	18.9173 0.0036	40	18.3808 0.0043	48	18.1880 0.0049		
30	VIDEO J022254.76-051213.4	35.7281547 -5.2037306	78	19.3492 0.0027	39	18.8672 0.0029	40	18.4067 0.0041	48	18.1372 0.0053		
31	VIDEO J022327.86-040627.2	35.8660837 -4.1075563	78	19.1724 0.0024	39	18.6624 0.0024	40	18.1648 0.0042	48	17.9286 0.0050		
32	VIDEO J022350.96-041325.5	35.9623324 -4.2237615	78	18.8035 0.0017	39	18.3172 0.0021	40	17.8155 0.0034	48	17.5798 0.0045		
33	VIDEO J022352.36-041526.6	35.9681759 -4.2573895	77	18.8680 0.0021	39	18.3799 0.0028	40	17.9367 0.0028	48	17.7016 0.0042		
34	VIDEO J022353.52-051217.0	35.9729949 -5.2047350	78	18.7733 0.0025	39	18.2901 0.0022	40	17.7774 0.0028	48	17.5529 0.0039		
35	VIDEO J022404.66-045222.2	36.0194131 -4.8728386	78	19.1804 0.0022	39	18.4466 0.0024	40	17.9480 0.0021	48	17.6283 0.0044		
36	VIDEO J022649.80-043149.0	36.7075066 -4.5302703	74	18.9232 0.0017	75	18.7517 0.0016	38	18.4144 0.0022	40	17.9624 0.0034	50	17.8677 0.0040
37	UCAL J055056.46+155253.9	87.7352518 15.8816295	106	17.2730 0.0070	121	17.0544 0.0035	136	16.6104 0.0031	132	16.2224 0.0041	136	16.0999 0.0060
38	UCAL J055210.55+161245.3	88.0439399 16.2125856	86	17.4837 0.0095	103	17.2840 0.0044	130	16.7693 0.0048	125	16.1954 0.0036	133	16.0186 0.0051
39	UltraVISTA J095849.29+022910.4	149.7053794 2.4862294		90	18.3682 0.0013	131	17.8524 0.0009	232	17.3109 0.0010	199	17.0759 0.0010	
40	UltraVISTA J095850.10+024719.9	149.7087571 2.7888722		75	18.4555 0.0011	80	17.9656 0.0008	123	17.4313 0.0012	101	17.2116 0.0018	

Table 7 – continued Standard Stars with VISTA-System ZYJHKs

VFS	IAU name	RA ^o Decl. ^o	n Z	Z n Y ± mag	Y n J ± mag	J n H ± mag	H n Ks ± mag	Ks ± mag
41	UltraVISTA J095853.62+024504.2	149.7234241 2.7511805		75 19.2576 0.0012	80 18.6410 0.0012	123 18.1390 0.0019	101 17.8376 0.0021	
42	UltraVISTA J095854.36+023524.9	149.7264829 2.5902461		140 18.3791 0.0013	150 17.8180 0.0007	236 17.2913 0.0011	203 17.0327 0.0012	
43	UltraVISTA J095855.38+024424.0	149.7307359 2.7399894		75 18.7503 0.0010	80 18.1943 0.0008	123 17.6766 0.0013	101 17.4237 0.0019	
44	UltraVISTA J095855.53+024134.4	149.7313560 2.6928870		143 18.0241 0.0008	158 17.5590 0.0006	252 17.0082 0.0009	206 16.7933 0.0009	
45	UltraVISTA J095855.67+024357.8	149.7319650 2.7327131		75 19.8434 0.0022	80 19.2441 0.0020	123 18.7651 0.0025	101 18.4652 0.0033	
46	UltraVISTA J095855.97+024741.0	149.7332239 2.7947267		71 18.4389 0.0009	78 17.8730 0.0008	120 17.4382 0.0013	97 17.1655 0.0016	
47	UltraVISTA J095856.54+021913.8	149.7355822 2.3205009		140 18.8246 0.0010	150 18.3514 0.0007	236 17.7820 0.0012	203 17.5625 0.0014	
48	UltraVISTA J095856.65+022914.1	149.7360512 2.4872598		147 18.0802 0.0008	152 17.6720 0.0006	232 17.0809 0.0009	199 16.9594 0.0010	
49	UltraVISTA J095859.43+024338.2	149.7476065 2.7272746		75 19.1804 0.0016	80 18.6534 0.0014	123 18.1630 0.0017	101 17.9131 0.0027	
50	UltraVISTA J095901.56+024340.8	149.7564883 2.7279976		75 17.9949 0.0011	80 17.4583 0.0008	123 16.8964 0.0010	101 16.6443 0.0012	
51	UltraVISTA J095902.34+024657.9	149.7597522 2.7827541		75 18.4764 0.0012	80 17.8232 0.0009	123 17.2872 0.0014	101 16.9664 0.0015	
52	UltraVISTA J095905.83+024007.4	149.7742789 2.6687115		79 18.2324 0.0011	104 17.8107 0.0008	251 17.2140 0.0010	206 17.0529 0.0010	
53	UltraVISTA J095906.54+024642.1	149.7772394 2.7783479		75 18.8640 0.0011	80 18.3290 0.0011	123 17.7934 0.0014	101 17.5463 0.0018	
54	UltraVISTA J095910.16+023459.8	149.7923194 2.5832843		140 18.1225 0.0012	150 17.5830 0.0006	237 17.1304 0.0011	203 16.8712 0.0010	
55	UltraVISTA J095915.75+024611.1	149.8156044 2.7697500		75 18.2690 0.0009	80 17.7772 0.0010	123 17.2745 0.0010	101 17.0546 0.0013	
56	UltraVISTA J095916.13+024618.3	149.8172140 2.7717426		75 18.2823 0.0009	80 17.8016 0.0008	123 17.2609 0.0013	101 17.0372 0.0014	
57	UltraVISTA J095918.04+024539.0	149.8251519 2.7608222		75 18.3345 0.0010	80 17.8417 0.0007	123 17.3732 0.0012	101 17.1457 0.0014	
58	UCAL J182653.41+040331.5	276.7225557 4.0587376	133 17.4972	131 17.2159 0.0081	156 16.6992 0.0042	157 16.1551 0.0036	167 15.9994 0.0034	
59	UCAL J182718.74+035838.7	276.8280740 3.9774041	140 17.2663	138 17.0325 0.0074	158 16.5879 0.0035	157 16.1728 0.0036	169 16.0038 0.0033	
60	UCAL J182857.59+040542.8	277.2399424 4.0952285	135 17.5724	137 17.2598 0.0085	156 16.7456 0.0041	154 16.3002 0.0037	168 16.0376 0.0037	
61	UCAL J182904.80+043119.7	277.2699877 4.5221425	135 17.6120	133 17.3401 0.0081	157 16.7872 0.0040	156 16.3344 0.0037	167 16.1180 0.0037	
62	UDXS J221217.08+004949.3	333.0711763 0.8303505			26 17.3587 0.0027		22 16.5811 0.0046	
63	UDXS J221217.17+005458.4	333.0715557 0.9162355			26 18.1551 0.0035		22 17.3931 0.0054	
64	UDXS J221217.24+011120.2	333.0718253 1.1889522			26 18.2026 0.0042		22 17.4465 0.0059	
65	UDXS J221308.15-002438.1	333.2839533 -0.4105822			24 17.7879 0.0030		27 17.0097 0.0048	
66	UDXS J221310.28+004403.5	333.2928434 0.7343005			24 17.4070 0.0028	29 16.9648 0.0033	24 16.6916 0.0048	
67	UDXS J221312.69+004516.1	333.3028790 0.7544734			24 17.5557 0.0035	29 17.1132 0.0037	24 16.8090 0.0054	
68	UDXS J221326.27+004504.4	333.3594622 0.7512320			24 18.3002 0.0034	29 17.8259 0.0034	24 17.5602 0.0057	
69	UDXS J221331.78+004432.8	333.3824122 0.7424491			24 17.8077 0.0028	28 17.3309 0.0037	24 16.9979 0.0048	
70	UDXS J221348.36+004340.2	333.4515020 0.7278254			24 17.6807 0.0044	29 17.2226 0.0032	24 16.9545 0.0049	
71	UDXS J221359.70+004405.8	333.4987510 0.7349581			24 17.9313 0.0034	29 17.4356 0.0043	24 17.1440 0.0052	
72	UDXS J221450.27+003128.5	333.7094552 0.5245924			25 17.2650 0.0024	27 16.6699 0.0032	22 16.5297 0.0064	
73	UDXS J221544.78-005649.9	333.9366041 -0.9471891			24 17.3086 0.0024		24 16.4942 0.0050	
74	UDXS J221835.85+012255.2	334.6493784 1.3819891			33 17.8448 0.0039	20 17.2731 0.0054	44 16.9818 0.0051	
75	UDXS J221916.37+002334.2	334.8182190 0.3928450			32 17.6622 0.0034		34 16.8747 0.0054	
76	UDXS J221942.03+004338.8	334.9251383 0.7274321			31 17.4172 0.0030	21 16.8889 0.0016	34 16.7754 0.0047	
77	UDXS J222007.27+002643.6	335.0303119 0.4454373			29 17.4399 0.0040	22 17.0128 0.0035	30 16.9227 0.0049	
78	UDXS J222153.93+003033.1	335.4746997 0.5091841			45 17.3604 0.0031	33 16.7993 0.0034	46 16.5495 0.0049	
79	UDXS J222205.63+001714.8	335.5234567 0.2874459			31 17.1721 0.0036	26 16.6742 0.0036	32 16.5423 0.0052	
80	UDXS J222219.75-000839.9	335.5823067 -0.1444080			28 17.3728 0.0031		33 16.6027 0.0042	
81	UDXS J222227.61+003032.8	335.6150576 0.5091194			31 17.2914 0.0027	26 16.8690 0.0036	32 16.7655 0.0054	

APPENDIX A: SQL QUERIES

SQL for the DXS

```

SELECT s.ra, s.dec, s.jAperMag3,v.jMeanMag,v.jnGoodObs,
s.jAperMag3err, v.jMagRms, v.jMagMAD,
s.hAperMag3,v.hMeanMag, v.hnGoodObs,
s.hAperMag3err,v.hMagRms, v.hMagMAD, s.kAperMag3,
v.kMeanMag, v.knGoodObs,s.kAperMag3err, v.kMagRms,
v.kMagMAD FROM dxsSource AS s, dxsVariabil-
ity AS v WHERE s.sourceID=v.sourceID AND
s.mergedClass=-1 AND v.variableClass=0 AND s.dec
> -30 AND v.kMeanMag>16.5 AND v.jnGoodObs>20
AND v.hnGoodObs>5 AND v.knGoodObs>20 AND
(v.jMagMAD/(SQRT(v.jnGoodObs - 1)))<=0.004
AND (v.hMagMAD/(SQRT(v.hnGoodObs - 1)))<=0.004
AND (v.kMagMAD/(SQRT(v.knGoodObs - 1)))<=0.004
AND (v.jMagRms/SQRT(v.jnGoodObs - 1))<=0.006
AND (v.hMagRms/SQRT(v.hnGoodObs - 1))<=0.006
AND (v.kMagRms/SQRT(v.knGoodObs - 1))<=0.006
AND ((s.jAperMag3 - v.jMeanMag) < 2.5 *
(SQRT(s.jAperMag3err * s.jAperMag3err
+ (v.jMagRms/SQRT(v.jnGoodObs - 1)) *
(v.jMagRms/SQRT(v.jnGoodObs - 1))))
AND ((s.hAperMag3 - v.hMeanMag) < 2.5 *
(SQRT(s.hAperMag3err * s.hAperMag3err
+ (v.hMagRms/SQRT(v.hnGoodObs - 1)) *
(v.hMagRms/SQRT(v.hnGoodObs - 1))))
AND ((s.kAperMag3 - v.kMeanMag) < 2.5 *
(SQRT(s.kAperMag3err * s.kAperMag3err
+ (v.kMagRms/SQRT(v.knGoodObs - 1)) *
(v.kMagRms/SQRT(v.knGoodObs - 1))))

```

SQL for the UDS

NOTE: there is an offset between AperMag3 and MeanMag due to the former not being aperture-corrected.

```

SELECT s.ra, s.dec, s.jAperMag3,v.jMeanMag,v.jnGoodObs,
s.jAperMag3err, v.jMagRms, v.jMagMAD,
s.hAperMag3,v.hMeanMag, v.hnGoodObs,
s.hAperMag3err,v.hMagRms, v.hMagMAD, s.kAperMag3,
v.kMeanMag, v.knGoodObs,s.kAperMag3err, v.kMagRms,
v.kMagMAD FROM udsSource AS s, udsVariability AS v
WHERE s.sourceID=v.sourceID AND s.mergedClass=-
1 AND v.variableClass=0 AND v.kMeanMag>17.5
AND v.jnGoodObs>100 AND v.hnGoodObs>100 AND
v.knGoodObs>100 AND (v.jMagMAD/(SQRT(v.jnGoodObs
- 1)))<=0.004 AND (v.hMagMAD/(SQRT(v.hnGoodObs
- 1)))<=0.004 AND (v.kMagMAD/(SQRT(v.knGoodObs
- 1)))<=0.004 AND (v.jMagRms/SQRT(v.jnGoodObs
- 1))<=0.006 AND (v.hMagRms/SQRT(v.hnGoodObs
- 1))<=0.006 AND (v.kMagRms/SQRT(v.knGoodObs
- 1))<=0.006 AND s.jAperMag3err<=0.003 AND
s.hAperMag3err<=0.003 AND s.kAperMag3err<=0.003
AND (s.jAperMag3 - v.jMeanMag < 0.20) AND
(s.jAperMag3 - v.jMeanMag > 0.18) AND (s.hAperMag3
- v.hMeanMag < 0.21) AND (s.hAperMag3 - v.hMeanMag
> 0.19) AND (s.kAperMag3 - v.kMeanMag < 0.19) AND
(s.kAperMag3 - v.kMeanMag > 0.17)

```

SQL for the UltraVISTA

NOTE: there is an offset between AperMag3 and MeanMag

due to differences in the aperture correction and zeropoints.

```

SELECT v.sourceID, s.ra, s.dec, v.variableClass,
s.yclassStat, s.jclassStat, s.hclassStat,
s.ksclassStat, s.yAperMag3, v.ymeanMag,
v.ynGoodObs, s.yAperMag3err, v.yMagRms,
v.yMagMAD, s.jAperMag3, v.jmeanMag, v.jnGoodObs,
s.jAperMag3err, v.jMagRms, v.jMagMAD, s.hAperMag3,
v.hmeanMag, v.hnGoodObs, s.hAperMag3err,
v.hMagRms, v.hMagMAD, s.ksAperMag3, v.ksmeanMag,
v.ksnGoodObs, s.ksAperMag3err, v.ksMagRms,
v.ksMagMAD FROM ultravistaSource AS s, ultrav-
istaVariability AS v WHERE s.sourceID=v.sourceID
AND v.variableClass=0 AND v.ksMeanMag > 16.5
AND s.hclassStat>0.7 AND s.ksclassStat>0.7
AND v.ynGoodObs>=20 AND v.jnGoodObs>=20 AND
v.hnGoodObs>=20 AND v.ksnGoodObs>=20 AND
(v.yMagMAD/(SQRT(v.ynGoodObs- 1)))<=0.004 AND
(v.jMagMAD/(SQRT(v.jnGoodObs- 1)))<=0.004 AND
(v.hMagMAD/(SQRT(v.hnGoodObs - 1)))<=0.004 AND
(v.ksMagMAD/(SQRT(v.ksnGoodObs- 1)))<=0.004
AND (v.yMagRms/SQRT(v.ynGoodObs- 1))<=0.006
AND (v.jMagRms/SQRT(v.jnGoodObs- 1))<=0.006
AND (v.hMagRms/SQRT(v.hnGoodObs- 1))<=0.006
AND (v.ksMagRms/SQRT(v.ksnGoodObs- 1))<=0.006
AND ((s.yAperMag3 - v.yMeanMag) <= 0.0) AND
((s.yAperMag3 - v.yMeanMag) >= -0.04) AND
((s.jAperMag3 - v.jMeanMag) <= -0.04) AND
((s.jAperMag3 - v.jMeanMag) >= -0.08) AND
((s.hAperMag3 - v.hMeanMag) <= 0.04) AND
((s.hAperMag3 - v.hMeanMag) >= 0.00) AND
((s.ksAperMag3 - v.ksMeanMag) <= 0.02) AND
((s.ksAperMag3 - v.ksMeanMag) >= -0.02)

```

SQL for VIDEO

```

SELECT v.sourceID, s.ra, s.dec, s.mergedClass,
s.zAperMag3, v.zMeanMag,v.znGoodObs,
s.zAperMag3err, v.zMagRms, v.zMagMAD,
s.yAperMag3,v.ymeanMag,v.ynGoodObs,s.yAperMag3err,
v.yMagRms, v.yMagMAD, s.jAperMag3,v.jmeanMag,v.jnGoodObs,
s.jAperMag3err, v.jMagRms, v.jMagMAD,
s.hAperMag3,v.hmeanMag,v.hnGoodObs,
s.hAperMag3err, v.hMagRms, v.hMagMAD,
s.ksAperMag3, v.ksmeanMag,
v.ksnGoodObs,s.ksAperMag3err, v.ksMagRms,
v.ksMagMAD FROM videoSource AS s, videoVariability
AS v WHERE s.sourceID=v.sourceID AND s.mergedClass
in (-1, -2) AND v.variableClass=0 AND s.dec > -
30 AND v.ksMeanMag > 17.5 AND v.ynGoodObs>20
AND v.jnGoodObs> 20 AND v.hnGoodObs > 20 AND
v.ksnGoodObs > 20 AND (v.yMagMAD/(SQRT(v.ynGoodObs
- 1)))<=0.004 AND (v.jMagMAD/(SQRT(v.jnGoodObs
- 1)))<=0.004 AND (v.hMagMAD/(SQRT(v.hnGoodObs -
1)))<=0.004 AND (v.ksMagMAD/(SQRT(v.ksnGoodObs
- 1)))<=0.004 AND (v.yMagRms/SQRT(v.ynGoodObs
- 1))<=0.006 AND (v.jMagRms/SQRT(v.jnGoodObs
- 1))<=0.006 AND (v.hMagRms/SQRT(v.hnGoodObs
- 1))<=0.006 AND (v.ksMagRms/SQRT(v.ksnGoodObs
- 1))<=0.006 AND ((s.yAperMag3 - v.yMeanMag)
< 2.5 * (SQRT(s.yAperMag3err * s.yAperMag3err
+ (v.yMagRms/SQRT(v.ynGoodObs - 1)) *
(v.yMagRms/SQRT(v.ynGoodObs - 1))))

```

```

AND ((s.jAperMag3 - v.jMeanMag) < 2.5 *
(SQRT(s.jAperMag3err * s.jAperMag3err
+ (v.jMagRms/SQRT(jnGoodObs - 1)) *
(v.jMagRms/SQRT(v.jnGoodObs - 1))))))
AND ((s.hAperMag3 - v.hMeanMag) < 2.5 *
(SQRT(s.hAperMag3err * s.hAperMag3err
+ (v.hMagRms/SQRT(v.hnGoodObs - 1)) *
(v.hMagRms/SQRT(v.hnGoodObs - 1)))))) AND
((s.ksAperMag3 - v.ksMeanMag) < 2.5 *
(SQRT(s.ksAperMag3err * s.ksAperMag3err
+ (v.ksMagRms/SQRT(ksnGoodObs - 1)) *
(v.ksMagRms/SQRT(ksnGoodObs - 1))))))

```

SQL for WFCAMCAL

```

SELECT s.ra, s.dec, s.zAperMag3,v.zMeanMag,v.znGoodObs,
s.zAperMag3err, v.zMagRms, v.zMagMAD,
s.yAperMag3,v.yMeanMag, v.ynGoodObs,
s.yAperMag3err, v.yMagRms, v.yMagMAD, s.jAperMag3,
v.jMeanMag,v.jnGoodObs, s.jAperMag3err, v.jMagRms,
v.jMagMAD, s.hAperMag3,v.hMeanMag,v.hnGoodObs,
s.hAperMag3err,v.hMagRms, v.hMagMAD, s.kAperMag3,
v.kMeanMag, v.knGoodObs,s.kAperMag3err,
v.kMagRms, v.kMagMAD FROM calSource AS s, cal-
Variability AS v WHERE s.sourceID=v.sourceID
AND s.mergedClass=-1 AND v.variableClass=0
AND v.kMeanMag>16 AND v.ynGoodObs>100 AND
v.jnGoodObs>100 AND v.hnGoodObs>100 AND
v.knGoodObs>100 AND (v.yMagMAD/(SQRT(v.ynGoodObs
- 1)))<=0.004 AND (v.jMagMAD/(SQRT(v.jnGoodObs
- 1)))<=0.004 AND (v.hMagMAD/(SQRT(v.hnGoodObs
- 1)))<=0.004 AND (v.kMagMAD/(SQRT(v.knGoodObs
- 1)))<=0.004 AND (v.yMagRms/SQRT(v.ynGoodObs
- 1))<=0.006 AND (v.jMagRms/SQRT(v.jnGoodObs
- 1))<=0.006 AND (v.hMagRms/SQRT(v.hnGoodObs
- 1))<=0.006 AND (v.kMagRms/SQRT(v.knGoodObs
- 1))<=0.006 AND ((s.yAperMag3 - v.yMeanMag)
< 2.5 * (SQRT(s.yAperMag3err * s.yAperMag3err
+ (v.yMagRms/SQRT(v.ynGoodObs - 1)) *
(v.yMagRms/SQRT(v.ynGoodObs - 1))))))
AND ((s.jAperMag3 - v.jMeanMag) < 2.5 *
(SQRT(s.jAperMag3err * s.jAperMag3err
+ (v.jMagRms/SQRT(v.jnGoodObs - 1)) *
(v.jMagRms/SQRT(v.jnGoodObs - 1))))))
AND ((s.hAperMag3 - v.hMeanMag) < 2.5 *
(SQRT(s.hAperMag3err * s.hAperMag3err
+ (v.hMagRms/SQRT(v.hnGoodObs - 1)) *
(v.hMagRms/SQRT(v.hnGoodObs - 1))))))
AND ((s.kAperMag3 - v.kMeanMag) < 2.5 *
(SQRT(s.kAperMag3err * s.kAperMag3err
+ (v.kMagRms/SQRT(v.knGoodObs - 1)) *
(v.kMagRms/SQRT(v.knGoodObs - 1))))))

```

APPENDIX B: POSSIBLE GALAXIES

**APPENDIX C: STARS EXCLUDED FROM THE
FINAL SAMPLE**

Table C1. Data for Sources Identified as Likely Stars with Atypical Colours

IR Survey Name	RA ^o Decl. ^o	Pan-STARRS meanPSF AB mags					VISTA Vega mags				
		<i>g</i> ± mag	<i>r</i> ± mag	<i>i</i> ± mag	<i>z</i> ± mag	<i>y</i> ± mag	<i>Z</i> ± mag	<i>Y</i> ± mag	<i>J</i> ± mag	<i>H</i> ± mag	<i>K_s</i> ± mag
UDS	34.2123189	21.7954	21.6093	20.3610	19.8250	19.4105					
	-4.8947515	0.1793	0.0835	0.0147	0.0315	0.1145			18.3512	17.8466	17.6092
UDS	34.4109253		21.7650	20.7175	19.9836	19.7015			0.0021	0.0019	0.0033
	-5.2700687		0.1675	0.0290	0.0255	0.0731			18.5133	18.0228	17.7496
UDS	34.5890235		21.8035	20.8665	20.1967	19.7849			0.0022	0.0019	0.0033
	-4.9424929		0.0724	0.0345	0.0278	0.0966			18.6272	18.1619	17.9030
VIDEO	35.1128282	21.6591	21.9368	20.8698	20.1845	19.8103			0.0021	0.0020	0.0033
	-4.9552726	0.1655	0.1798	0.0538	0.0102	0.0657			19.1399	18.6294	18.1766
VIDEO	52.0756099				20.8638	19.9288			0.0020	0.0025	0.0028
	-27.8683759				0.0682	0.0791	20.2966	19.4553	18.6419	18.1248	17.7045
DXS	333.3096800		21.6666	20.8225	20.1457	19.7224	0.0063	0.0043	0.0026	0.0037	0.0050
	0.7372219		0.1489	0.0248	0.0391	0.0516			18.3903	17.8713	17.5302
DXS	333.8609666		21.4346	20.2861	19.5578	19.1589			0.0040	0.0053	0.0051
	0.7496622		0.1123	0.0126	0.0266	0.2435			18.0057	17.4381	17.1374
									0.0055	0.0036	0.0047

Table C2. Likely Stars with Deviant Mean and Aperture Magnitudes

Survey	RA ^o Decl. ^o	<i>Z</i> mean ± mag	<i>Z</i> Aper ± mag	<i>Y</i> mean ± mag	<i>Y</i> Aper ± mag	<i>J</i> mean ± mag	<i>J</i> Aper ± mag	<i>H</i> mean ± mag	<i>H</i> Aper ± mag	<i>K</i> (s) mean ± mag	<i>K</i> (s) Aper ± mag
VIDEO	35.1191358			19.2971	19.2615	18.8033	18.8031	18.3092	18.3053	18.0712	18.0743
	-4.4549895			0.0025	0.0093	0.0037	0.0086	0.0035	0.0082	0.0045	0.0090
CAL	87.6786696	17.4104	17.5649	17.2602	17.2153	16.7709	16.7628	16.1723	16.1782	16.0033	16.0350
	15.8554744	0.0039	0.0183	0.0031	0.0153	0.0037	0.0172	0.0034	0.0138	0.0036	0.0211
CAL	276.8783681	17.3634	17.3458	17.0501	17.0870	16.5950	16.6020	16.0855	16.0882	16.0014	15.9022
	4.5214510	0.0031	0.0159	0.0028	0.0144	0.0030	0.0167	0.0027	0.0148	0.0040	0.0218
CAL	277.1729349	17.5923	17.6030	17.3352	17.3172	16.8237	16.8150	16.3529	16.2602	16.1989	16.0637
	4.5807735	0.0035	0.0184	0.0028	0.0159	0.0035	0.0180	0.0031	0.0161	0.0050	0.0242

APPENDIX D: FINDING CHARTS

This paper has been typeset from a $\text{T}_{\text{E}}\text{X}/\text{L}^{\text{A}}\text{T}_{\text{E}}\text{X}$ file prepared by the author.

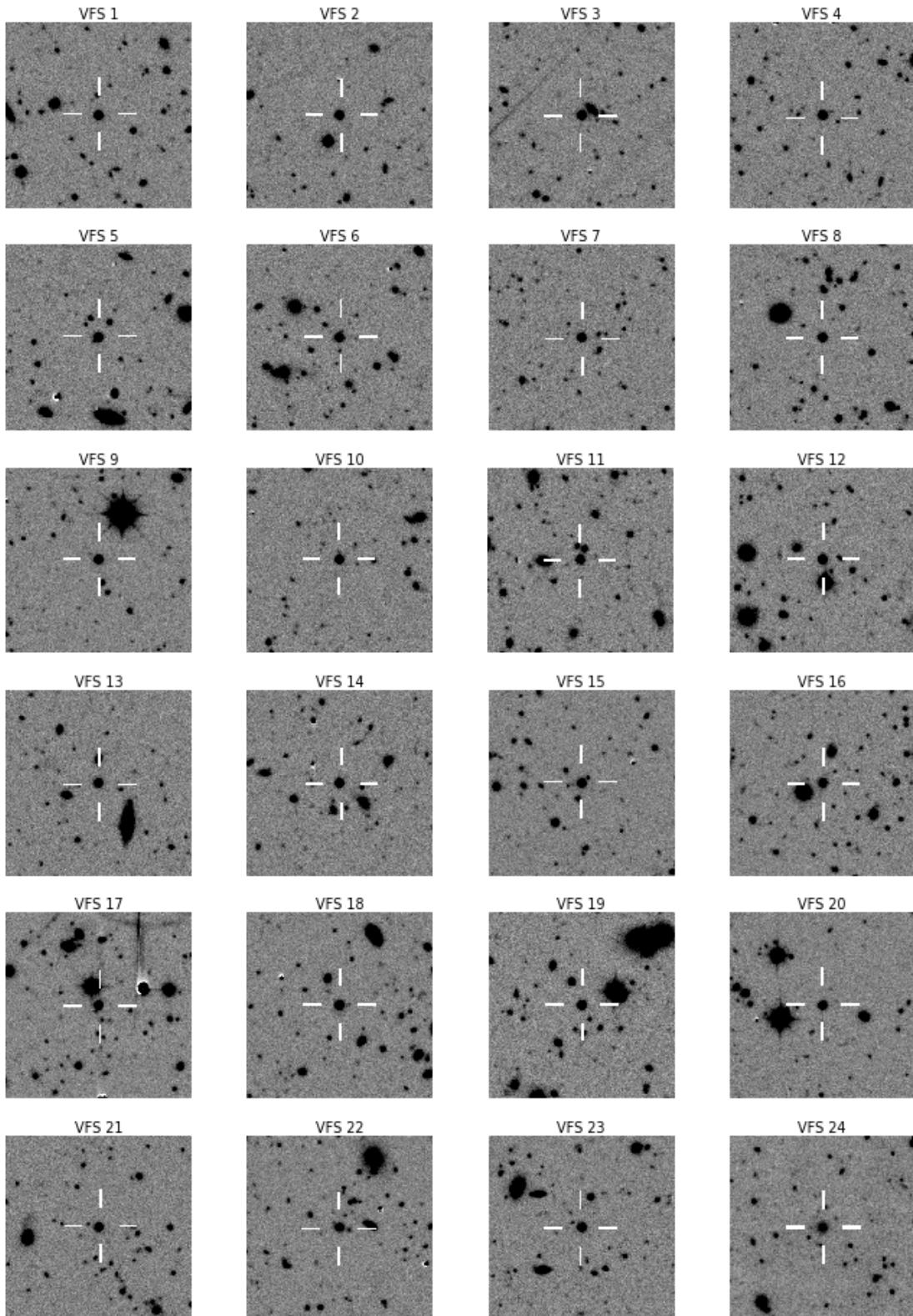


Figure D1. J-band finding charts, 1 arcminute field-of-view, for the standards presented above in Table 7. North is up and east to the left.

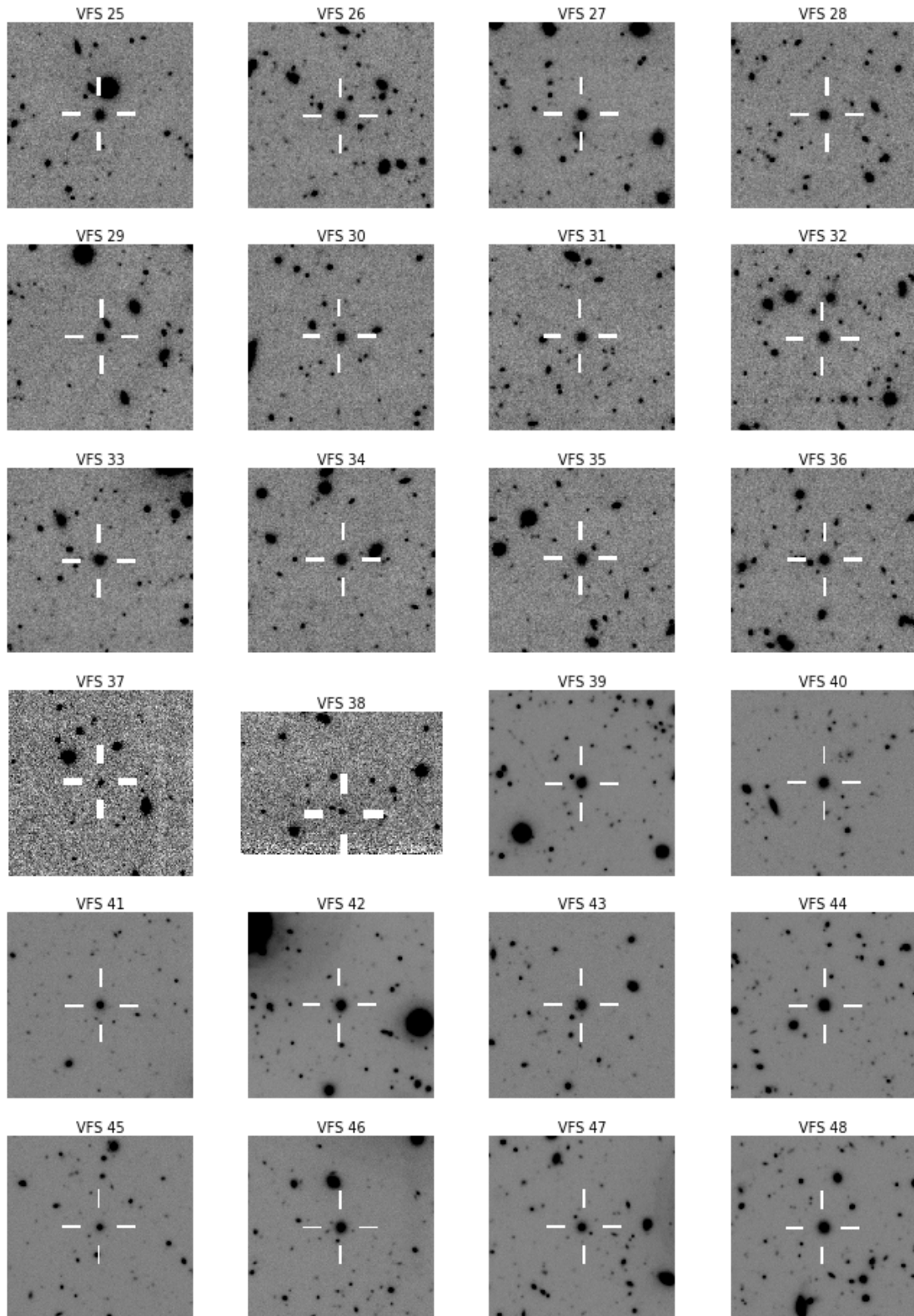


Figure D1. (cont.) J-band finding charts, 1 arcminute field-of-view, for the standards presented above in Table 7. North is up and east to the left.

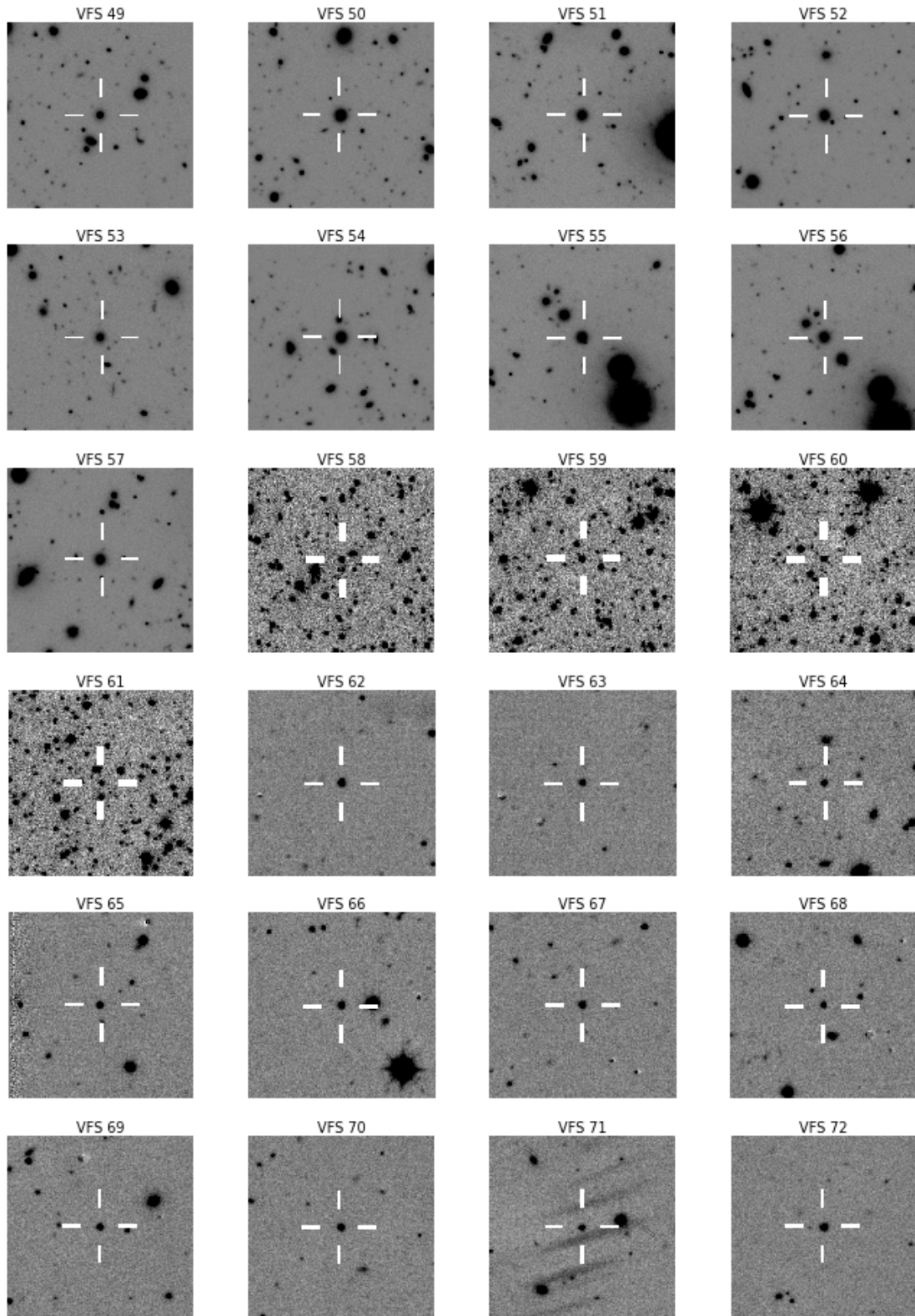


Figure D1. (cont.) J-band finding charts, 1 arcminute field-of-view, for the standards presented above in Table 7. North is up and east to the left.

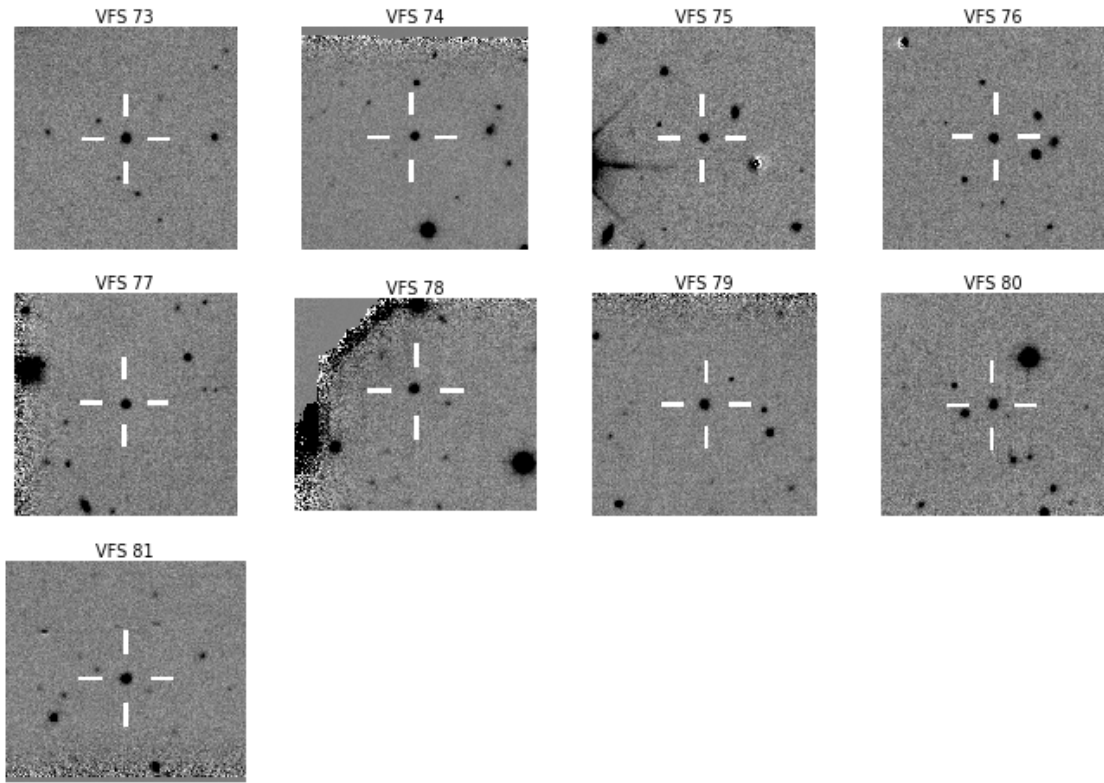


Figure D1. (cont.) J-band finding charts, 1 arcminute field-of-view, for the standards presented above in Table 7. North is up and east to the left.